Analysis of glycosaminoglycan synthesis in cartilage explant. We analyzed glycosaminoglycan synthesis in cartilage explants as previously described[14], except that we used a Sephacryl S500HR column whose length and diameter were 30 cm and 1 cm, respectively (GE Healthcare) in **Figure 2e**. We cultured rib cartilage from three embryos at 18.5 dpc in DMEM with [^{35}S]sulfate (GE Healthcare) to label the glycosaminoglycan sulfate residues. Proteoglycan fractions were obtained from cultures through extraction with 4 M guanidine hydrochloride and purification by Q-Sepharose (GE Healthcare) column chromatography. We then measured the molecular size of proteoglycan and glycosaminoglycan in the proteoglycan fractions with gel-filtration chromatography.

Disaccharide compositional analysis. We prepared lyophilized humerus and femur for disaccharide compositional analysis. After exhaustive enzymatic digestion of partially purified glycosaminoglycans with a mixture of chondroitinase and heparitinase, we determined the unsaturated disaccharide composition by fluorometric postcolumn HPLC[13] with chondroitin sulfate- (Seikagaku Corporation) and heparan sulfate–derived (Sigma-Aldrich) unsaturated disaccharide standards.

Human subjects. We screened for *SLC35D1* mutations in six individuals with Schneckenbecken dysplasia who were registered in the International Skeletal Dysplasia Registry, the European Sustainable Development Network and the Japanese Skeletal Dysplasia Consortium; three had typical and three had possible Schneckenbecken dysplasia (**Supplementary Table 2**). Samples were obtained after informed consent. All procedures were conducted according to the protocols and guidelines approved by the participating institutions. Brief summaries of the findings in the two subjects with *SLC35D1* mutations are provided in the **Supplementary Case Report**.

Mutation screening. We isolated genomic DNAs by using standard procedures and examined *SLC35D1* for mutations by PCR from genomic DNA followed by direct sequencing. We amplified the 12 exons of *SLC35D1* with their flanking intron sequences by PCR and sequenced the products with an ABI Prism 3700 automated sequencer (PE Biosystems). PCR conditions and primer sequences are available upon request.

RT-PCR analysis. We extracted total RNA from the frozen chondro-osseous tissue of Subject 2 by using ISOGEN (Nippongene) and synthesized random-primed cDNAs with the TaqMan Multiscribe Reverse kit (Applied Biosystems). To examine the effect of the IVS7+1G→T mutation on RNA splicing, we amplified a *SLC35D1* cDNA segment spanning exons 5–9 with the primer pair 5′-TCTGAGAAGGTTCTCCATCC-3′ and 5′-AGAAGAAAGAGGGTGTCAGC-3′. To examine whether mutations in Subject 2 were compound heterozygous, we amplified a cDNA segment spanning exons 7–12 with the primer pair 5′-TTGGCATTTGATCTGGAAGGA-3′ and 5′-TATACCAGGCTCCCAGCAAT-3′. We subcloned RT-PCR products with the TOPO TA Cloning Kit (Invitrogen) and sequenced them.

Nucleotide-sugar transporter activity. We measured the NST activity of SLC35D1 mutants with a heterologous expression system in *Saccharomyces cerevisiae* as previously described[4,5]. We constructed pYEX-BESN3 expression vectors encoding N-terminal hemagglutinin epitope–tagged wild-type and mutant SLC35D1 proteins. We prepared microsome fractions from cells expressing wild-type and mutant SLC35D1 and measured the amount of radiolabeled nucleotide-sugar incorporated into the fractions.

Note: Supplementary information is available on the Nature Medicine website.

ACKNOWLEDGMENTS

We thank M. Nakayama (Kazusa DNA Research Institute) for donating the ES cell–BAC library. We are grateful to M. Muraoka for measurement of NST activity, to I. Kataoka and Y. Mizutani-Koseki for their assistance in histochemical analysis and *in situ* hybridization and to S. Tominaga for her help in genetic analysis of the human *SLC35D1*. This project was supported by Special Coordination Funds for the Promotion of Science and Technology from the Japanese Ministry of Education, Culture, Sports, Science and Technology (Contract Grant No. 13043003 to H.K.) and by grants-in-aid from the Ministry of Education, Culture, Sports and Science of Japan (Contract Grant No. 19209049), Research on Child Health and Development (Contract Grant Nos. 17C-1 and H18-005 to S.I.), the Ministry of Education, Culture, Sports and Science of Japan (Contract Grant No. 19510205 to S.H.) and the US National Institutes of Health (HD22657 and MO1-RR00425 to D.H.C. and D.L.R.). D.H.C. is the recipient of a Winnick Family Clinical Scholar Award.

AUTHOR CONTRIBUTIONS

S.H. and T.F. performed the main experiments, analyzed data and prepared the manuscript. G.N., D.L.R., A.S.-F., P.G.N. and D.H.C. recruited human subjects and analyzed the human phenotypic data. S.S. and M.Y. performed proteoglycan analysis in knockout mice. M.O. and K.K. generated knockout mice and carried out histological analysis. H.T. and A.K.-T. determined glycosaminoglycan content. N.I., K.I. and Y.S. assayed mouse Slc35d1 protein. H.K. and S.I. planned and supervised the mouse and human parts of the project, respectively.

Published online at http://www.nature.com/naturemedicine
Reprints and permissions information is available online at http://npg.nature.com/reprintsandpermissions

1. Knudson, C.B. & Knudson, W. Cartilage proteoglycans. *Semin. Cell Dev. Biol.* **12**, 69–78 (2001).
2. Schwartz, N.B. & Domowicz, M. Chondrodysplasias due to proteoglycan defects. *Glycobiology* **12**, 57R–68R (2002).
3. Sugahara, K. & Kitagawa, H. Recent advances in the study of the biosynthesis and functions of sulfated glycosaminoglycans. *Curr. Opin. Struct. Biol.* **10**, 518–527 (2000).
4. Muraoka, M., Kawakita, M. & Ishida, N. Molecular characterization of human UDP-glucuronic acid/UDP-N-acetylgalactosamine transporter, a novel nucleotide sugar transporter with dual substrate specificity. *FEBS Lett.* **495**, 87–93 (2001).
5. Muraoka, M., Miki, T., Ishida, N., Hara, T. & Kawakita, M. Variety of nucleotide sugar transporters with respect to the interaction with nucleoside mono- and diphosphates. *J. Biol. Chem.* **282**, 24615–24622 (2007).
6. Plaas, A.H., Wong-Palms, S., Roughley, P.J., Midura, R.J. & Hascall, V.C. Chemical and immunological assay of the nonreducing terminal residues of chondroitin sulfate from human aggrecan. *J. Biol. Chem.* **272**, 20603–20610 (1997).
7. Superti-Furga, A. *et al.* Achondrogenesis type IB is caused by mutations in the diastrophic dysplasia sulphate transporter gene. *Nat. Genet.* **12**, 100–102 (1996).
8. Hastbacka, J. *et al.* Atelosteogenesis type II is caused by mutations in the diastrophic dysplasia sulfate transporter gene (DTDST): evidence for a phenotypic series involving three chondrodysplasias. *Am. J. Hum. Genet.* **58**, 255–262 (1996).
9. ul Haque, M.F. *et al.* Mutations in orthologous genes in human spondyloepimetaphyseal dysplasia and the brachymorphic mouse. *Nat. Genet.* **20**, 157–162 (1998).
10. Thiele, H. *et al.* Loss of chondroitin 6-*O*-sulfotransferase-1 function results in severe human chondrodysplasia with progressive spinal involvement. *Proc. Natl. Acad. Sci. USA* **101**, 10155–10160 (2004).
11. Kluppel, M., Wight, T.N., Chan, C., Hinek, A. & Wrana, J.L. Maintenance of chondroitin sulfation balance by chondroitin-4-sulfotransferase 1 is required for chondrocyte development and growth factor signaling during cartilage morphogenesis. *Development* **132**, 3989–4003 (2005).
12. Ishida, N. & Kawakita, M. Molecular physiology and pathology of the nucleotide sugar transporter family (SLC35). *Pflugers Arch.* **447**, 768–775 (2004).
13. Toyoda, H., Kinoshita-Toyoda, A. & Selleck, S.B. Structural analysis of glycosaminoglycans in *Drosophila* and *Caenorhabditis elegans* and demonstration that tout-velu, a *Drosophila* gene related to EXT tumor suppressors, affects heparan sulfate *in vivo*. *J. Biol. Chem.* **275**, 2269–2275 (2000).
14. Ogihara, Y. *et al.* Biosynthesis of proteoglycan in bone and cartilage of parathyroid hormone–related protein knockout mice. *J. Bone Miner. Metab.* **19**, 4–12 (2001).
15. Borochowitz, Z. *et al.* A distinct lethal neonatal chondrodysplasia with snail-like pelvis: Schneckenbecken dysplasia. *Am. J. Med. Genet.* **25**, 47–59 (1986).
16. Giedion, A. *et al.* Case report 693. *Skeletal Radiol.* **20**, 534–538 (1991).
17. Nikkels, P.G., Stigter, R.H., Knol, I.E. & van der Harten, H.J. Schneckenbecken dysplasia, radiology and histology. *Pediatr. Radiol.* **31**, 27–30 (2001).
18. Superti-Furga, A. & Unger, S. Nosology and classification of genetic skeletal disorders: 2006 revision. *Am. J. Med. Genet. A.* **143**, 1–18 (2007).
19. Thomsen, B. *et al.* A missense mutation in the bovine SLC35A3 gene, encoding a UDP-N-acetylglucosamine transporter, causes complex vertebral malformation. *Genome Res.* **16**, 97–105 (2006).
20. Joyner, A.L. *Gene Targeting* 1–146 (Oxford University Press, Oxford, UK, 1992).
21. Kessel, M. & Gruss, P. Homeotic transformations of murine vertebrae and concomitant alteration of Hox codes induced by retinoic acid. *Cell* **67**, 89–104 (1991).
22. Kessel, M. & Gruss, P. Murine developmental control genes. *Science* **249**, 374–379 (1990).
23. Shibata, S., Fukada, K., Imai, H., Abe, T. & Yamashita, Y. *In situ* hybridization and immunohistochemistry of versican, aggrecan and link protein, and histochemistry of hyaluronan in the developing mouse limb bud cartilage. *J. Anat.* **203**, 425–432 (2003).
24. Wallin, J. *et al.* The role of Pax-1 in axial skeleton development. *Development* **120**, 1109–1121 (1994).

Development 134, 579-590 (2007) doi:10.1242/dev.02747

Mammalian Polycomb Scmh1 mediates exclusion of Polycomb complexes from the XY body in the pachytene spermatocytes

Yuki Takada[1], Kyo-ichi Isono[1], Jun Shinga[1], James M. A. Turner[2], Hiroshi Kitamura[1], Osamu Ohara[1], Gen Watanabe[3], Prim B. Singh[4], Takehiko Kamijo[5], Thomas Jenuwein[6], Paul S. Burgoyne[2] and Haruhiko Koseki[1,*]

The product of the Scmh1 gene, a mammalian homolog of *Drosophila* Sex comb on midleg, is a constituent of the mammalian Polycomb repressive complexes 1 (Prc1). We have identified Scmh1 as an indispensable component of the Prc1. During progression through pachytene, Scmh1 was shown to be excluded from the XY body at late pachytene, together with other Prc1 components such as Phc1, Phc2, Rnf110 (Pcgf2), Bmi1 and Cbx2. We have identified the role of Scmh1 in mediating the survival of late pachytene spermatocytes. Apoptotic elimination of *Scmh1*$^{-/-}$ spermatocytes is accompanied by the preceding failure of several specific chromatin modifications at the XY body, whereas synapsis of homologous autosomes is not affected. It is therefore suggested that Scmh1 is involved in regulating the sequential changes in chromatin modifications at the XY chromatin domain of the pachytene spermatocytes. Restoration of defects in *Scmh1*$^{-/-}$ spermatocytes by *Phc2* mutation indicates that Scmh1 exerts its molecular functions via its interaction with Prc1. Therefore, for the first time, we are able to indicate a functional involvement of Prc1 during the meiotic prophase of male germ cells and a regulatory role of Scmh1 for Prc1, which involves sex chromosomes.

KEY WORDS: Mouse, Polycomb, Scmh1, Spermatogenesis, Apoptosis, XY body

INTRODUCTION

The Polycomb group (PcG) genes were first identified by their requirement for the maintenance of the stable repression of Hox genes during the development of *Drosophila melanogaster* (Jürgens, 1985; Paro, 1995; Pirrotta, 1997). *Drosophila* PcG gene products form large multimeric protein complexes and are thought to act by changing the local chromatin structure, as suggested by the synergistic genetic interactions between mutant alleles of different *Drosophila* PcG genes (Jürgens, 1985; Franke et al., 1992; Paro, 1995; Pirrotta, 1997; Shao et al., 1999). In mammals, genes structurally and functionally related to *Drosophila* PcG genes have been identified and mammalian PcG gene products form several distinct complexes. Polycomb repressive complex-2 (Prc2), which contains the product of Eed (the ortholog of the *Drosophila* extra sex combs gene), Ezh2 (the ortholog of the *Drosophila* enhancer of zeste gene) and Suz12, mediates trimethylation of histone H3 at K27 (H3-K27) by Ezh2 component (Schumacher et al., 1996; Laible et al., 1997; van Lohuizen et al., 1998; Sewalt et al., 1998; van der Vlag and Otte, 1999). The second complex, which is closely related to the Polycomb repressive complex-1 (Prc1) in *Drosophila*, includes the products of the paralogs of class 2 PcG genes (Levine et al., 2002). This subset contains gene groups, namely *Pcgf2* (also known as *Rnf110* and *Mel18*, and hereafter referred to as *Rnf110*) and *Bmi1*, *Cbx2* (also known as *M33*), *Cbx4* (also known as *MPc2*) and *Cbx8* (also known as *Pc3*), *Phc1* (also known as *rae28*), *Phc2* and *Phc3*, *Ring1* and *Rnf2* (also known as *Ring1B*) (Levine et al., 2002). The Prc1 complex is compositionally and functionally conserved between flies and mammals (Shao et al., 1999; Levine et al., 2002; Gebuhr et al., 2000). In mammals, chromatin binding of Prc1 involves its recognition of trimethylated H3-K27 (Boyer et al., 2006; Lee et al., 2006; Fujimura et al., 2006). The Prc1 complex has a significant impact on the control of not only anteroposterior (AP) specification of the axis via Hox regulation, but also the proliferation and senescence via regulation of the Ink4a/p53 pathway (Jacobs et al., 1999).

Sex comb on midleg (*Scm*) gene is a member of *Drosophila PcG* genes and, based on database comparison, its product contains three separable functional domains (Bornemann et al., 1996), namely: a pair of N-terminal zinc fingers, two tandem 100-amino acid repeats, called mbt repeats as they are also found in the fly tumor suppressor encoded by the *l(3)mbt* [*lethal(3) malignant brain tumor*] gene, and C-terminal homology domain of 65 amino acids, called the SPM domain. The SPM domain is a self-binding protein interaction module and may mediate Scm association to Prc1 and play a key role for PcG repression, although Scm association to purified Prc1 is substoichiometric (Levine et al., 2002). In mammals, there are four paralogs for *Drosophila Scm* based on primary sequence: *Scmh1*, *Scml1*, *Scml2* and *Sfmbt* (Tomotsune et al., 1999; van de Vosse et al., 1998; Montini et al., 1999; Usui et al., 2000). The mammalian Scmh1 protein has been shown to be a constituent of the mammalian Prc1 (Levine et al., 2002), which contains two highly conserved motifs, two mbt repeats in the N-terminal region and an SPM domain in the C-terminal region, that are shared with its *Drosophila* counterpart. The SPM domain of Scmh1 can mediate its

[1]RIKEN Research Center for Allergy and Immunology, 1-7-22 Suehiro, Tsurumi-ku, Yokohama 230-0045, Japan. [2]Division of Stem Cell Research and Developmental Genetics, MRC National Institute for Medical Research, The Ridgeway, Mill Hill, London NW7 1AA, UK. [3]Laboratory of Veterinary Physiology, Tokyo University of Agriculture and Technology, Fuchu, Tokyo 183-8509, Japan. [4]Nuclear Reprogramming Laboratory, Division of Gene Expression and Development, Roslin Institute (Edinburgh), Roslin, Midlothian EH25 9PS, UK. [5]Department of Pediatrics, Shinshu University School of Medicine, Matsumoto, Nagano 390-8621, Japan. [6]Research Institute of Molecular Pathology, The Vienna Biocenter, Dr Bohrgasse 7, A-1030 Vienna, Austria.

*Author for correspondence (e-mail: koseki@rcai.riken.jp)

Accepted 17 November 2006

interaction with *Drosophila* polyhomeotic (Ph) and mammalian Phc1 and Phc2, through their respective SPM domains (Tomotsune et al., 1999). It is also notable that tissue-specific *Scmh1* mRNA levels in the testes are the highest of all tissues analyzed and they increase during the synchronous progression of first-wave spermatogenesis in parallel with *Phc1* (see Fig. S1A,B in the supplementary material). These observations suggest a role of mammalian Prc1 during spermatogenesis.

Before the specialized cell division of meiosis, postmitotic spermatocytes enter into an extended meiotic prophase, in which homologous autosomal chromosomes pair and undergo reciprocal recombination. There is accumulating evidence to suggest that the quality of this complex process is monitored by a checkpoint to ensure spermatogenic success, as represented by the apoptotic elimination of those spermatocytes with synaptic errors. During this period, heteromorphic sex chromosomes pair only in a small pseudoautosomal region (PAR) at their distal ends and undergo transcriptional inactivation, termed meiotic sex chromosome inactivation (MSCI), by remodeling into heterochromatin, thus forming the XY body (Perry et al., 2001; Odorisio et al., 1996; Singer-Sam et al., 1990; Turner et al., 2004; Baarends et al., 1999; Strahl and Allis, 2000; Turner et al., 2000; Hoyer-Fender et al., 2000; Mahadevaiah et al., 2001; Khalil et al., 2004). Formation of the XY body is conserved throughout the mammalian phylogenetic tree and is therefore assumed to be essential for successful spermatogenesis and the faithful segregation of sex chromosomes. Indeed, in mutants for the gene encoding histone H2A.X and the tumor suppressor protein Brca1, failure to form the XY body coincides with sterility due to the apoptotic elimination of such mutant spermatocytes before completion of meiosis (Fernandez-Capetillo et al., 2003; Xu et al., 2003). However, it has not been definitely demonstrated that spermatogenic arrest in these mutants is because of failure to form the XY body or due to some other reason. The condensation of the X and Y chromosome to form the XY body is associated with post-translational modifications of histones and the recruitment or exclusion of various chromatin-associated proteins (Turner et al., 2001; Hoyer-Fender et al., 2000; Richler et al., 2000; Mahadevaiah et al., 2001; Khalil et al., 2004; Baarends et al., 1999; Baarends et al., 2005). Early in the formation of the XY body, phosphorylated histone H2A.X (γH2A.X) and ubiquitylated histone H2A (uH2A) are enriched at the XY body and then X and Y chromosomes undergo sequential changes in their histone modifications, which correlate with transcriptional status of sex chromosomes (Mahadevaiah et al., 2001; Baarends et al., 1999; Baarends et al., 2005). The functional involvement of these histone modifications at the XY body was properly addressed for the first time in a study using *Brca1* mutants, in which H2A.X phosphorylation was shown to be essential to trigger MSCI (Turner et al., 2004). However, the roles of hyperubiquitylation of H2A on the X and Y chromosomes have still not been addressed. Recent studies have revealed an Rnf2 component of Prc1 to be an E3 component of ubiquitin ligase for histone H2A to link Prc1 with the XY body (de Napoles et al., 2004; Baarends et al., 1999; Baarends et al., 2005).

In this study, we have generated a mouse line carrying a mutant *Scmh1* allele that lacks the exons to encode an SPM domain. Axial homeotic transformations and premature senescence in mouse embryonic fibroblasts (MEFs) in the homozygotes indicated the role of Scmh1 as a PcG component. Approximately half the $Scmh1^{-/-}$ males were infertile, which correlates with an accelerated apoptosis of postmitotic pachytene spermatocytes. The present genetic study indicates the involvement of Prc1 during XY body maturation and the regulatory role of Scmh1 gene products in the exclusion of Prc1 from the XY body, which may in turn be required for the further progression of meiotic prophase.

MATERIALS AND METHODS

Mice

Scmh1-deficient mice were generated using R1 embryonic stem (ES) cells according to the conventional protocol and backcrossed to C57BL/6 background four to six times (Akasaka et al., 1996). Schematic representations of genomic organization and targeting vector are shown in Fig. S2 in the supplementary material. *Scmh1* mutant mice were genotyped by PCR using the following oligonucleotides: (a) 5′-GTCAG-GTGTGCCCGCTACTGT-3′ and (b) 5′-GATGGATTGCACGCAGGTTC-3′ for the mutant allele; and (a) and (c) 5′-GGCCGACTAGGC-CATCTTCTG-3′ for the *Scmh1* wild-type allele. As *Scmh1* and *Phc2* loci were on chromosome 4 and 28×10^6 base pairs (bp) apart from each other, we first generated recombinants in which *Scmh1* and *Phc2* mutant alleles were physically linked. This double mutant allele was used to generate *Scmh1;Phc2* double homozygotes. Skeletal analysis was performed as described previously (Kessel and Gruss, 1991). MEFs were maintained according to a 3T9 protocol as described previously (Kamijo et al., 1997).

In situ hybridization, RT-PCR and immunohistochemistry

In situ hybridization was performed as described previously (Yuasa et al., 1996). The nucleotide sequences of the primers used for RT-PCR in this study are listed in Table 1. Immunohistochemistry was performed as described previously (Hoyer-Fender et al., 2000).

TUNEL staining

Apoptotic cells were visualized by the terminal deoxynucleotidetransferase-mediated dUTP nick end-labeling (TUNEL) assay (In Situ Cell Death Detection Kit, AP; Roche, Germany).

Immunocytochemistry of spread spermatocytes

Meiotic prophase cell spreads and squashes were prepared as described previously (Scherthan et al., 2000). After washing with PBS for 3 minutes, slides bearing cell spreads were processed for immunostaining using standard procedures. The antibodies used for immunostaining in this study are listed in Table 2. For the statistical analyses, 300 spermatocytes derived from five mice with respective genotypes were analyzed and the significance was further analyzed by *t*-test.

Microarray analysis

Microarray analysis was performed using Mouse Genome 430 2.0 GeneChips (Affymetrix, Santa Clara, CA) according to the manufacturer's instructions. The intensity for each probe set was calculated using the MAS5 method of the GCOS software package (Affymetrix) at the default setting. Per chip normalization was performed using a median correction program in the GeneSpring software package (Agilent Technologies, Palo Alto, CA). One comparison between the two groups was conducted using a triplicate array. Data of probe sets were excluded from the analyses when they were judged to be 'absent' by the GCOS program in at least one sample in the stimulated groups. Probe sets that differentially hybridized between the samples were identified by the following criteria: (1) Welch's analysis of variance (ANOVA) showed that the *P*-value was less than 0.05; (2) the Benjamini and Hochberg false discovery test confirmed the ANOVA result; and (3) more than a twofold difference in the expression levels was observed between the samples.

RESULTS

Scmh1 is a functional component of PcG complexes

We generated a mutant allele for Scmh1 by deleting the sequences encoding the SPM domain, in which a small amount of truncated *Scmh1* transcript was expressed (see Fig. S2A-E in the supplementary material). As the *Drosophila* Scm^{XF24} allele, in which the SPM domain is exclusively affected, presents an almost identical phenotype to null alleles, the *Scmh1* mutant allele could be a null or

Table 1. Primers used in semiquantitative RT-PCR analyses

Gene	Forward (5'→3')	Reverse (5'→3')
A-myb	aagaagttggttgaacaacacgg	aggaagtaacttagcaatctcgg
Dmc1	ttcgtactggaaaaactcagctgtatc	cttggctgcgacataatcaagtagctcc
Mvh1	ccaaaagtgacatatataccc	ttggttgatcacttctcgag
Scp-3	ggtggaagaaagcattctgg	cagctccaaatttttccagc
CyclinA1	atgcatcgccagagctccaagag	ggaagtggagatctgacttgagc
Calmegin	atatgcgtttccagggtgttggac	gtatgcacctccacaatcaatacc
Bmp8a	ggctcgagatggtggtcaaggcctgtgg	ggggatccaggctctttctatgtggcc
CREMτ	gattgaagaagaaaaatcaga	catgctgtaatcagttcatag
β-actin	gagagggaaatcgtgcgtga	acatctgctggaaggtggac
Scmh1		
Primers 1/2	atgctggtttgctac	aggacaaaggtttcacct
Primers 3/4	actgccacagagtataatca	tcagaacttgccctg

Table 2. Antibodies used in immunostaining analyses

Antibody	Species	Dilution	Company
Anti-p53(clone pAb421)	Rabbit	1:500	Oncogene Research Products
Anti-Scp3	Rabbit	1:100	Novus Biologicals
Anti-phospho-H2A.X (Ser139)	Rabbit	1:500	Upstate
Anti-ubiquityl-Histone H2A(clone E6C5)	Mouse	1:100	Upstate
Anti-monomethyl-Histone H3(Lys9)	Rabbit	1:100	Upstate
Anti-dimethyl-Histone H3(Lys9)	Rabbit	1:100	Upstate
Anti-acetyl-Histone H3	Rabbit	1:100	Upstate
Anti-trimethyl-Histone H3 (Lys27)	Rabbit	1:100	Upstate
Anti-dimethyl-Histone H4 (Lys20)	Rabbit	1:100	Upstate
Anti-monomethyl-Histone H3 (Lys4)	Rabbit	1:100	Upstate
Anti-Rad51 (H-92)	Rabbit	1:50	Santa Cruz
Anti-Mlh1 (G168-15)	Mouse	1:50	BD Pharmingen
Anti-phosphorylated RNA polymerase II	Mouse	1:25	Covance
Anti-Scmh1	Mouse	Undiluted	This study
Anti-Phc1	Mouse	Undiluted	Miyagishima et al., 2003
Anti-Phc2	Mouse	Undiluted	Isono et al., 2005
Anti-Bmi1(H-99)	Rabbit	1:25	Santa Cruz
Anti-Rnf110(C-20)	Rabbit	1:30	Santa Cruz
Anti-Cbx2(C-18)	Rabbit	1:25	Santa Cruz
Anti-Rnf2	Mouse	Undiluted	Atsuta et al., 2001
Anti-Ezh2	Rabbit	1:100	Upstate
Anti-mouse IgM FITC	Donkey	1:100	Becton Dickinson
Anti-mouse IgG Cy2	Donkey	1:100	Jackson ImmunoResearch Laboratories
Anti-rabbit IgG Cy3	Donkey	1:500	Jackson ImmunoResearch Laboratories
Anti-mouse IgG (H+L) Alexa Fluor 488	Goat	1:300	Molecular Probes
Anti-rabbit IgG (H+L) Alexa Fluor 568	Goat	1:300	Molecular Probes
Anti-rabbit IgG, HRP-conjugated	Goat	1:2000	Amersham

strong hypomorphic mutation (Bornemann et al., 1996). Although both male and female *Scmh1*$^{-/-}$ mice were viable and grew normally to adulthood, homozygotes exhibited the axial homeosis and premature senescence of MEFs in the homozygous mutants, which was restored by the *p19*^{ARF} or *p53* mutation (see Fig. S2F-K in the supplementary material). Therefore, Scmh1 is an indispensable component of Prc1 in mice.

The expression and subcellular localization of Scmh1 during spermatogenesis

About half the homozygotes were sterile and had slightly smaller testes than their wild-type littermates (Y.T., unpublished). Before studying the pathogenesis of infertility in *Scmh1* mutants, we examined Scmh1 expression during spermatogenesis by in situ hybridization and immunohistochemical analysis. *Scmh1* expression was seen in the seminiferous tubules and interstitial cells (Fig. 1Aa). In the seminiferous tubules, morphological examination of the germ cell layers representing meiotic spermatocytes (particularly those at the pachytene stage) revealed that these germ layers were expressing the highest amount of *Scmh1*, with the least amounts expressed in spermatogonia and round spermatids (Fig. 1Ab). Sertoli cells also expressed a significant amount of *Scmh1*. By using an immunohistochemical technique, a light staining of the whole nucleus was observed in the zygotene stage and in more advanced cells up to pachytene spermatocytes (Fig. 1Ba). In addition, focal localization of Scmh1 was seen in the chromocenter of round spermatids (Fig. 1Bb). Concordantly, *Scmh1* expression in the testes correlated with synchronous progression of the first-wave spermatogenesis (see Fig. S1B in the supplementary material). From day 15 post partum (pp) onwards, the amount of *Scmh1* transcript progressively increased and reached a maximum level by day 25 pp. Taken together, *Scmh1* and its products are predominantly expressed in postmitotic spermatocytes.

We went on to investigate subcellular localization of Scmh1 by using spread meiotic spermatocytes. The synaptonemal complex protein Scp3, which is a component of the axial element, was used to substage meiosis (Xu et al., 2003). Scmh1 staining was seen in the nucleus as a diffused pattern from leptotene to early pachytene spermatocytes (Fig. 1Ca-c and Y.T., unpublished). In late pachytene spermatocytes, Scmh1 staining was significantly excluded from the

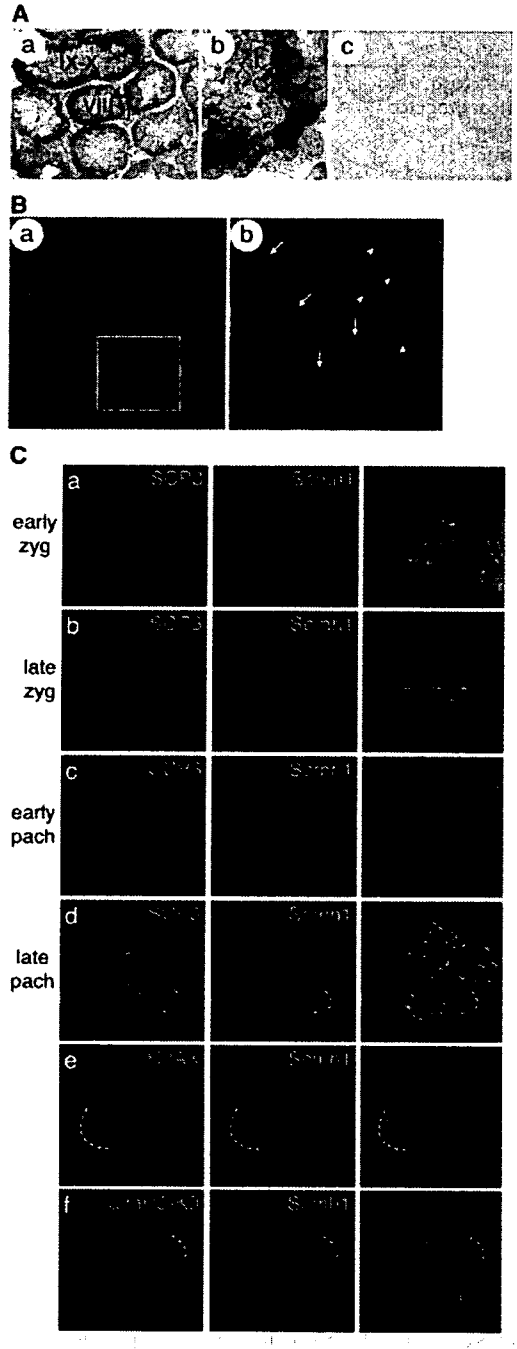

Fig. 1. Localization of Scmh1 in the adult testes and spermatocytes. (**Aa**) In situ hybridization using antisense probe. Stages of seminiferous tubules are given. (**Ab**) Higher magnification view of seminiferous tubule at stage VII shown in a. Arrows and arrowheads indicate pachytene spermatocytes and round spermatids, respectively. (**Ac**) Control slides using sense probe. (**Ba**) Immunohistochemical localization of Scmh1 of wild-type testes. (**Bb**) Higher magnification view of seminiferous tubule shown in a. Arrows and arrowheads indicate pachytene spermatocytes and round spermatids, respectively. (**C**) Immunocytochemical detection of Scmh1 gene products from zygotene to pachytene stage spermatocytes, which were prepared from day 18 pp wild-type testes. (**Ca-Cd**) Spermatocyte spreads were substaged into early (a) and late (b) zygotene and early (c) and late (d) pachytene stages based on anti-Scp3 (red) immunostaining and morphology. Scmh1 (green) was localized in the nuclei at each stage, but was mostly excluded from the X and Y chromosome territory at late pachytene stage, as indicated by dotted lines. (**Ce**) Reciprocal subnuclear localization of Scmh1 and γH2A.X indicated exclusion of Scmh1 from the XY body. The XY body is indicated by dotted lines. (**Cf**) Reciprocal subnuclear localization of Scmh1 and dimethylated H3-K9 indicated exclusion of Scmh1 from the XY body. The XY body is indicated by dotted lines.

XY chromatin domain (Fig. 1Cd,e). Concordantly, reciprocal localization of Scmh1 and γH2A.X was seen in about 80% of pachytene spermatocytes (Fig. 1Ce). Consistently, Scmh1 was excluded from the XY body in which dimethylated histone H3 at K9 (H3-K9) was enriched (Fig. 1Cf).

Subcellular localization of PcG proteins and trimethylated H3-K27 during spermatogenesis

The progressive exclusion of Scmh1 from the XY body during the pachytene stage prompted us to examine the subcellular localization of other PcG proteins and trimethylated H3-K27, which is mediated by the Ezh2 component of Prc2. Subcellular localization of Phc1, Phc2, Bmi1, Rnf110 and Cbx2 were compared with γH2A.X or uH2A. Reciprocal localization of these PcG proteins and γH2A.X or uH2A, within about 80% of spermatocytes, indicated the exclusion of other PcG proteins from the XY body during the pachytene stage, as well as Scmh1 (Fig. 2Aa-e). Consistently, Phc2 was excluded from the XY body in 77% of spermatocytes, in which dimethylated H3-K9 was enriched (Fig. 2Af). Taken together, PcG complexes are excluded from the XY body at the late pachytene stage almost concurrently with hyperdimethylation of H3-K9 at the XY body, whereas they are continuously present in the autosomal regions.

Recent studies have repeatedly provided evidence indicating the engagement of Prc1 by trimethylated H3-K27 mediated by Prc2 (Cao et al., 2002; Kuzmichev et al., 2002). We thus addressed whether the exclusion of Prc1 components from the XY body was correlated with the degree of H3-K27 trimethylation at the XY chromatin domain. Trimethylated H3-K27 was distributed throughout the nucleus as a diffuse pattern from leptotene to zygotene stage spermatocytes despite the fact that the signals were very dim (Fig. 2Ba and Y.T., unpublished). In early pachytene spermatocytes, trimethylated H3-K27 staining was much stronger than in the earlier stages but was significantly excluded from the XY chromatin domain (Fig. 2Bb). In late pachytene spermatocytes, its exclusion from the XY body was still maintained (Fig. 2Bc). Therefore the exclusion of trimethylated H3-K27 from the XY chromatin domain precedes those of Prc1 components.

Impaired spermatogenesis in *Scmh1*$^{-/-}$ males

We first examined the histology of *Scmh1*$^{-/-}$ testes in day 35 pp testes and revealed that about two-thirds were morphologically altered to varying extents. The seminiferous tubules of *Scmh1*$^{-/-}$ testes exhibited a reduction in the number of spermatocytes and a lack of spermatids and mature spermatozoa (Fig. 3Aa,b). Sertoli cells and spermatogonia were morphologically and numerically normal. Mono- or multinuclear large cells were sometimes seen. One-third of *Scmh1*$^{-/-}$ testes were morphologically indistinguishable from wild type. Therefore, spermatogenesis was variably affected in *Scmh1*$^{-/-}$ testes.

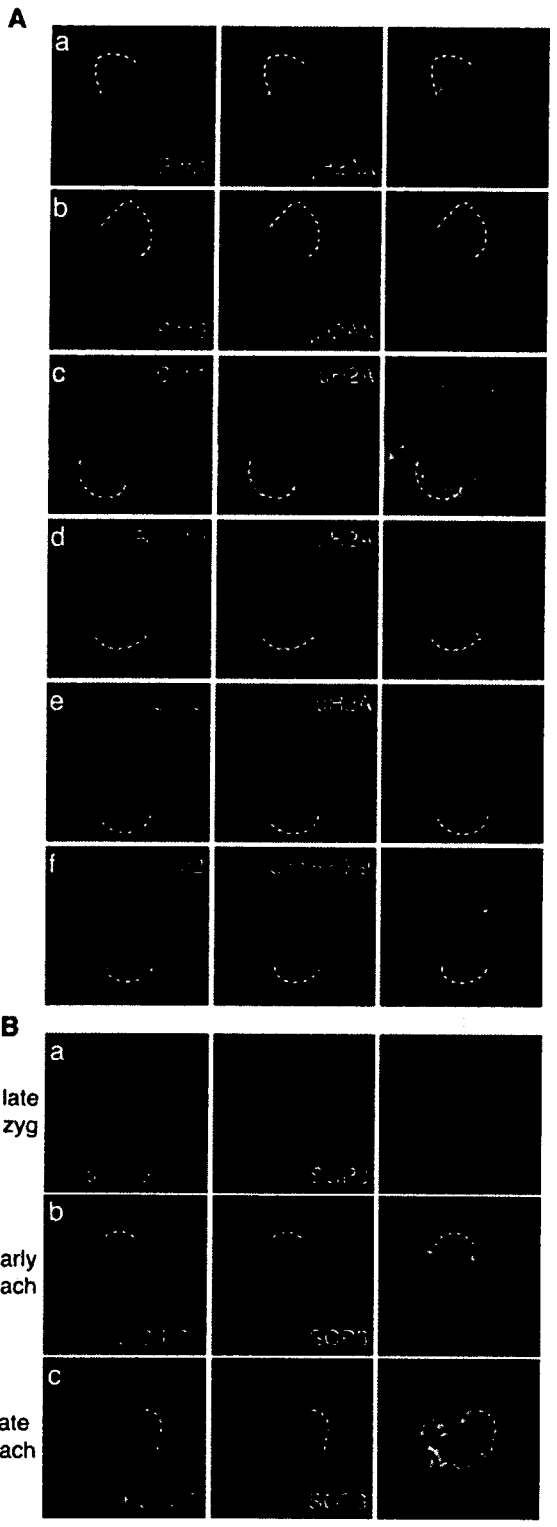

Fig. 2. Expression pattern of other PcG proteins and trimethylated H3-K27 at pachytene stage spermatocytes. (**A**) Immunocytochemical detection of Prc1 components in pachytene spermatocytes. (**Aa,Ab**) Phc1 (a) and Phc2 (b) were excluded from the XY body demarcated by extensive accumulation of γH2A.X. (**Ac-Ae**) Bmi1 (c), Rnf110 (d) and Cbx2 (e) were excluded from the XY body demarcated by extensive accumulation of uH2A. The XY body is indicated by dotted lines. (**Af**) Reciprocal subnuclear localization of Phc2 and dimethylated H3-K9 indicated exclusion of Scmh1 from the XY body. (**B**) Immunocytochemical detection of trimethylated H3-K27 from late zygotene to pachytene stage spermatocytes. Spermatocytes were immunostained by using anti-trimethylated H3-K27 (red) and anti-SCP3 (green). The X and Y chromosome territory is indicated by dotted lines.

We then examined *Scmh1*$^{-/-}$ testicular histology at various stages of first-wave spermatogenesis. Neither day 7 pp nor day 11 pp mutant mice exhibited any significant differences compared to wild type (Fig. 3B). The morphological changes in *Scmh1*$^{-/-}$ testes were observed in the seminiferous tubules as early as day 15 pp. At day 15 pp, most of the seminiferous tubules contained spermatogonia, Sertoli cells and several degenerating pachytene spermatocytes, whereas pre-leptotene to zygotene spermatocytes were seen rarely (see Fig. S3 in the supplementary material). Vacuoles were frequently seen in the luminal region. Based on these morphological parameters, days 15, 19, 25 and 30 pp testes were also examined. In conclusion, *Scmh1*$^{-/-}$ testes were progressively affected during first-wave spermatogenesis (Fig. 3B).

We went on to investigate the frequency of apoptosis during the progression of spermatogenesis by TUNEL labeling. In wild-type day 15 and 19 pp testes, a few TUNEL-labeled cells were clearly present but were seen only rarely in day 7 pp (Fig. 3Ca-c). In *Scmh1*$^{-/-}$ testes, a significant number of TUNEL-labeled cells were observed in the inner layers of seminiferous tubules at day 15 and 19 pp, but not at day 7 pp (Fig. 3Cd-h). These histological observations confirmed that postmitotic spermatocytes in meiotic prophase were predominantly affected in *Scmh1*$^{-/-}$ testes.

Finally, the expression of stage-specific molecular markers were examined by means of semi-quantitative RT-PCR analysis in wild-type and *Scmh1*$^{-/-}$ testes at day 35 pp, in order to address which stage of spermatogenesis was predominantly deleted in affected homozygous mutants (Fig. 3D). *CyclinA1*, *calmegin*, *Bmp8a* and *CREMτ* genes were used as markers for pachytene stage spermatocytes (Sweeney et al., 1996; Watanabe et al., 1994; Zhao and Hogan, 1996; Foulkes et al., 1992). These were reduced more than threefold in *Scmh1*$^{-/-}$ when compared with testes from wild type. In *Scmh1*$^{-/-}$ testes no change was observed in the expression of *A-myb*, *Dmc1*, *Mvh1* and *Scp3*, which are expressed before the pachytene stage (Mettus et al., 1994; Habu et al., 1996; Fujiwara et al., 1994; Tanaka et al., 2000; Klink et al., 1997). Taken together, in *Scmh1*$^{-/-}$ testes, postmitotic spermatocytes are predominantly depleted by apoptotic outbursts.

Apoptotic elimination of late pachytene spermatocytes occurs after synapsis of homologous chromosomes in *Scmh1*$^{-/-}$ testes

In order to further identify the meiotic substage at which *Scmh1*$^{-/-}$ spermatocytes are predominantly affected, immunolocalization studies were carried out in spread spermatogenic cells, prepared from day 18 pp males, by using antibodies against uH2A, γH2A.X and Scp3. Accumulation of uH2A on the XY body was seen in pachytene spermatocytes, whereas γH2A.X demarcates the XY body from late zygotene to diplotene stage (Baarends et al., 1999; Baarends et al., 2005; Mahadevaiah et al., 2001; Fernandez-

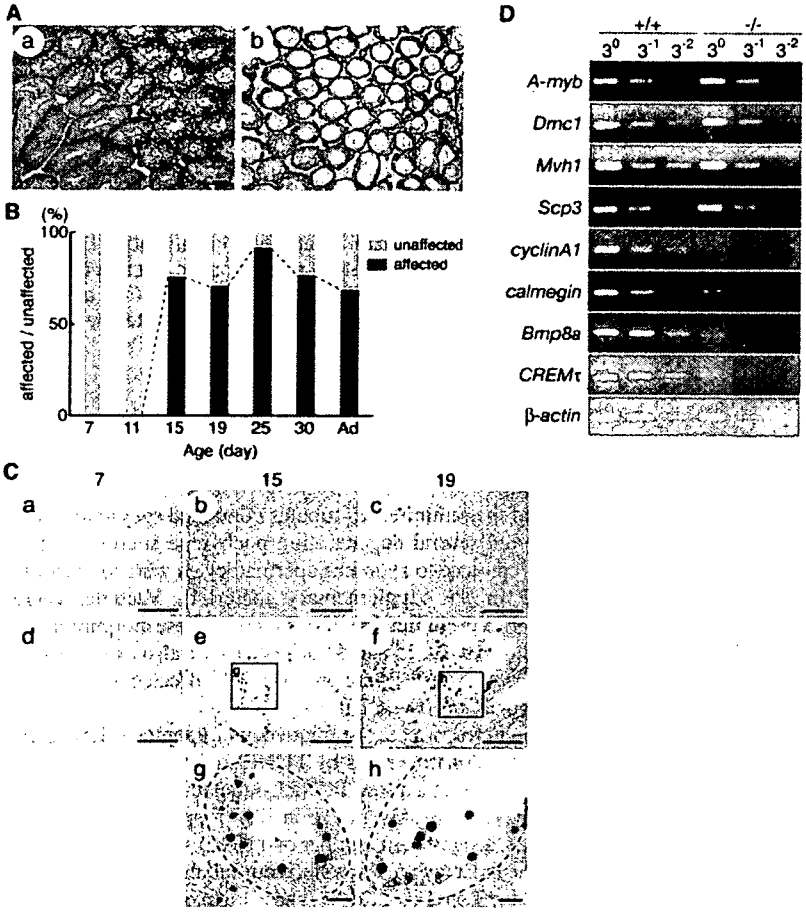

Fig. 3. Testicular abnormalities in *Scmh1*$^{-/-}$ mice. (**A**) Cross-sections of testes from day 35 pp wild-type (**Aa**) and *Scmh1*$^{-/-}$ (**Ab**) mice. Sections were stained with Hematoxylin and Eosin (HE). (**B**) The frequency of *Scmh1*$^{-/-}$ mice in which seminiferous tubules were morphologically affected during first-wave spermatogenesis. Days after birth are shown. At each age, more than ten mutants were examined. Mutants over 8 weeks of age were collected and indicated as adults (Ad). (**C**) Increased apoptotic spermatocytes in *Scmh1*$^{-/-}$ testes. (**Ca-Cc**) Incidence of apoptosis in wild-type testes at day 7, 15 and 19 pp. (**Cd-Cf**) Incidence of apoptosis in *Scmh1*$^{-/-}$ testes at day 7, 15 and 19 pp. (**Cg,Ch**) Higher magnification views of individual seminiferous tubules shown in e and f. Outline of seminiferous tubules are indicated by dotted lines. (**D**) The expression of stage-specific markers during spermatogenesis in wild-type and unaffected and affected *Scmh1*$^{-/-}$ testes at day 35 pp, as revealed by semi-quantitative RT-PCR. *β-actin* was used as a standard to verify the equal amounts of cDNA. Primers used in each reaction are shown in Table 1. Scale bars: 100 μm in A,B,Ca-Cf; 10 μm in Cg,Ch.

Capetillo et al., 2003; Xu et al., 2003). In particular, the degree of uH2A association to the XY body was intriguing, as the Rnf2 component of class 2 PcG has been shown to be an E3 component of ubiquitin ligase for histone H2A (Wang et al., 2004; de Napoles et al., 2004). We did not see any significant difference between *Scmh1*$^{-/-}$ and wild-type testes in the frequency of the spermatocytes, in which uH2A and γH2A.X localized on the XY bodies. This implies entry into pachytene stage was not affected in *Scmh1*$^{-/-}$ (Y.T., unpublished). Using Scp3 staining and morphology, we substaged further the spermatocytes, in which uH2A was accumulated on the XY body, into early and late pachytene stages (Fig. 4A). The frequency of early pachytene spermatocytes was 37% in wild type and 66% in *Scmh1*$^{-/-}$ (Fig. 4A). This suggests that *Scmh1*$^{-/-}$ spermatocytes were incompletely depleted by late pachytene.

During meiosis, synapsis is essential for proper chromosome segregation, and is monitored by various meiotic checkpoints (Cohen and Pollard, 2001). As proper chromosome alignment and segregation in the first meiotic division are ensured by recombination between homologous chromosomes, we examined the localization of Mlh1, a mismatch-repair protein, that forms foci at sites of meiotic crossover in mid- to late-pachytene spermatocytes (Celeste et al., 2002). Mlh1 foci were distributed on the synaptonemal complexes in late pachytene spermatocytes of both wild type and *Scmh1*$^{-/-}$ (Fig. 4B). Consistent with this observation, late pachytene spermatocytes remained in *Scmh1*$^{-/-}$ testes exhibited normal Scp3 distribution, including PAR of sex chromosomes (see Fig. S4 in the supplementary material). Taken together, Scmh1 is dispensable for pairing and synapsis of homologous chromosomes.

The role of Scmh1 at the XY body in pachytene spermatocytes

Apart from homologous autosomes, the X and Y chromosomes pair along PAR and undergo extensive and sequential remodeling into heterochromatin, thus forming the XY body, which is associated with transcriptional inactivation. Failure to form the XY body has been shown to coincide with male sterility and arrest of spermatogenesis, although it is not yet definitely proven whether the XY body is required for survival and fertility of male germ cells (Fernandez-Capetillo et al., 2003). Scmh1 and other PcG components were excluded at the transition from early to late pachytene stage. *Scmh1*$^{-/-}$ spermatocytes were affected at a stage that was temporally similar to that concerning the exclusion of PcG proteins from the XY chromatin domain. These observations prompted us to focus on whether spermatogenic arrest in *Scmh1*$^{-/-}$ testes is accompanied by changes in chromatin remodeling at the XY body. We first examined the degree of H3-K9 methylation, acetylation and phosphorylated RNA pol II association to the XY bodies, which have been shown to change during the pachytene stage (Richler et al., 2000; Khalil et al., 2004). In wild type, 76 and 62% of the XY body marked by uH2A were hyperdi- and hypermonomethylated at H3-K9, respectively, compared with 36 and 18%, respectively, in *Scmh1*$^{-/-}$ testes (Fig. 5Aa,b).

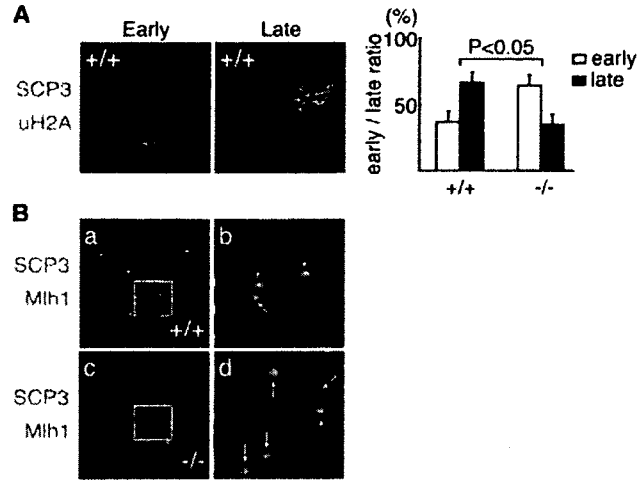

Fig. 4. Significant reduction of late pachytene spermatocytes in *Scmh1*$^{-/-}$ testes. (**A**) Reduction of late pachytene spermatocytes in spermatocyte spread prepared from day 18 pp *Scmh1*$^{-/-}$ testes in comparison with wild type. Spermatocytes were immunostained using anti-Scp3 (red) and uH2A (green). (Left) Wild-type spermatocytes, in which uH2A is enriched at the XY body, were examined at early or late pachytene stage, based on Scp3 immunostaining and morphology. (Right) Frequency of early and late pachytene spermatocytes was compared between the wild-type and *Scmh1*$^{-/-}$ testes. (**B**) Localization of Mlh1 in spermatocytes. (**Ba**) Spermatocytes of wild type were immunostained by using anti-Scp3 (red) and Mlh1 (green). (**Bb**) Higher magnification view of chromosomes shown in a. (**Bc**) Localization of Mlh1 in *Scmh1*$^{-/-}$ mutant testes. (**Bd**) Higher magnification view of chromosomes shown in c. Arrows in b and d indicate Mlh1 foci.

Phosphorylated RNA pol II was excluded from the XY body in 51% of the *Scmh1*$^{-/-}$ spermatocytes compared with 90% of wild type (Fig. 5Ac) (Richler et al., 2000; Khalil et al., 2004). These results suggest that elimination of late pachytene spermatocytes in *Scmh1*$^{-/-}$ testes is coincidental with the stage at which the XY body undergoes chromatin remodeling. It is also noteworthy that underacetylation of H3-K9 at the XY body was observed to a similar extent between the wild-type and *Scmh1*$^{-/-}$ spermatocytes (Fig. 5Ad). Changes in such specific chromatin modifications at the XY body of *Scmh1*$^{-/-}$ spermatocytes imply that they may not solely represent their developmental arrest at late pachytene stage. We therefore postulated a regulatory role for Scmh1 in sequential chromatin modifications of the XY body.

To address this possibility, we extended the analyses to other epigenetic modifications, which could potentially be influenced by *Scmh1* mutation. We first examined the localization of PRC1 components and trimethylated H3-K27, which was bound by PRC1, in *Scmh1*$^{-/-}$ testes. The frequency of meiotic spermatocytes exhibiting reciprocal localization of Phc1 or Phc2 and γH2A.X in *Scmh1*$^{-/-}$ spermatocytes was examined. In 79% of wild-type spermatocytes, Phc1 and Phc2 were excluded from the XY body demarcated by γH2A.X (Fig. 5Ba,b). In *Scmh1*$^{-/-}$ spermatocytes, the frequency of spermatocytes in which Phc1 and Phc2 were excluded from the XY body was reduced to 40 and 27%, respectively (Fig. 5Ba,b). Similarly, trimethylated H3-K27 was excluded from the XY body demarcated by uH2A in 88% of wild-type spermatocytes compared with 39% in *Scmh1*$^{-/-}$ spermatocytes (Fig. 5Bc). Therefore meiotic spermatocytes, in which the sequential exclusion of trimethylated H3-K27 and Prc1 components from the XY body had failed, may be predominantly depleted in *Scmh1*$^{-/-}$ testes. As the exclusion of trimethylated H3-K27 from the XY body is shown to precede the exclusion of PRC1 components in wild type, this result could be interpreted as recurrence of H3-K27 trimethylation in the late pachytene stage. We therefore substaged the spermatocytes in which trimethylated H3-K27 was excluded from the XY body into early and late pachytene stages by using Scp3 staining and morphology. In early pachytene stage, trimethylated H3-K27 was excluded from the XY body to a similar extent between the wild type and *Scmh1*$^{-/-}$ (Fig. 5Bd). In contrast, the frequency of late pachytene spermatocytes, in which trimethylated H3-K27 was excluded, was significantly reduced in *Scmh1*$^{-/-}$ testes compared to wild type (Fig. 5Bd). This suggests that Scmh1 is required to maintain the exclusion of trimethylated H3-K27 from the XY body in late pachytene spermatocytes but not in early pachytene.

We went on to examine the localization of monomethylated histone H3 at K4 (H3-K4) and dimethylated histone H4 at K20 (H4-K20) because the mbt repeats, which are also found in the Scmh1 N-terminal, have been shown to exhibit specific binding to mono- and dimethylated H3-K9, monomethylated H3-K4 and mono- and dimethylated H4-K20 (Kim et al., 2006; Klymenko et al., 2006). Neither hypermonomethylation of H3-K4 nor underdimethylation of H4-K20 at the XY body were significantly different between wild-type and *Scmh1*$^{-/-}$ spermatocytes (Fig. 5Ca,b). It is particularly noteworthy that H4-K20 underdimethylation at the XY body, which was exclusively seen in the late pachytene spermatocytes in wild type, was not affected in the mutants (Y.T., unpublished). Taken together, these results show that apoptotic elimination of late pachytene spermatocytes in *Scmh1*$^{-/-}$ testes is preceded by failure in hypermethylation of H3-K9, exclusion of phosphorylated RNA pol II and Prc1 components and undermethylation of H3-K27 at the XY body, whereas it is not accompanied by changes in H3-K9 acetylation or methylation of H3-K4 or H4-K20. These results support the idea that changes in chromatin modifications at the XY body of *Scmh1*$^{-/-}$ spermatocytes are not simply a consequence of apoptotic elimination of late pachytene spermatocytes. Instead, Scmh1 was suggested to play the regulatory role for the sequential changes in chromatin modifications of the XY body.

Phc2 mutation alleviates spermatogenic defects in *Scmh1*$^{-/-}$ spermatocytes

We postulated that Scmh1 functions via its direct interaction with Prc1 in pachytene spermatocytes, as Scmh1 has been identified as a constituent of Prc1 components because, in general, mutant interactions of *PcG* alleles have been shown to modify the respective phenotypes in mammals as well (Bel et al., 1998; Akasaka et al., 2001; Isono et al., 2005). We have generated *Scmh1;Phc2* double mutants (dko) as Phc2 protein binds to Scmh1 via its SPM domain and the homozygous mutants were viable and fertile (Isono et al., 2005) (Y.T., unpublished). dko mice were viable and born according to the principles of Mendelian inheritance, although some of them exhibited growth retardation (Y.T., unpublished). The fertility of ten normal-sized dko and *Scmh1*$^{-/-}$ males was tested by natural mating to approximately 10-week-old C57BL/6 females. Strikingly, all the dko males were fertile, whereas half the *Scmh1*$^{-/-}$ males were sterile (Fig. 6B). Histological inspections revealed that all the dko testes were morphologically indistinguishable from wild type at day 35 pp and the frequency of apoptotic outbursts in dko was significantly reduced in comparison with littermate *Scmh1*$^{-/-}$ testes (Fig. 6A,C). Significant restorations of late pachytene spermatocytes were also revealed by substaging spermatocytes using antibodies against di-

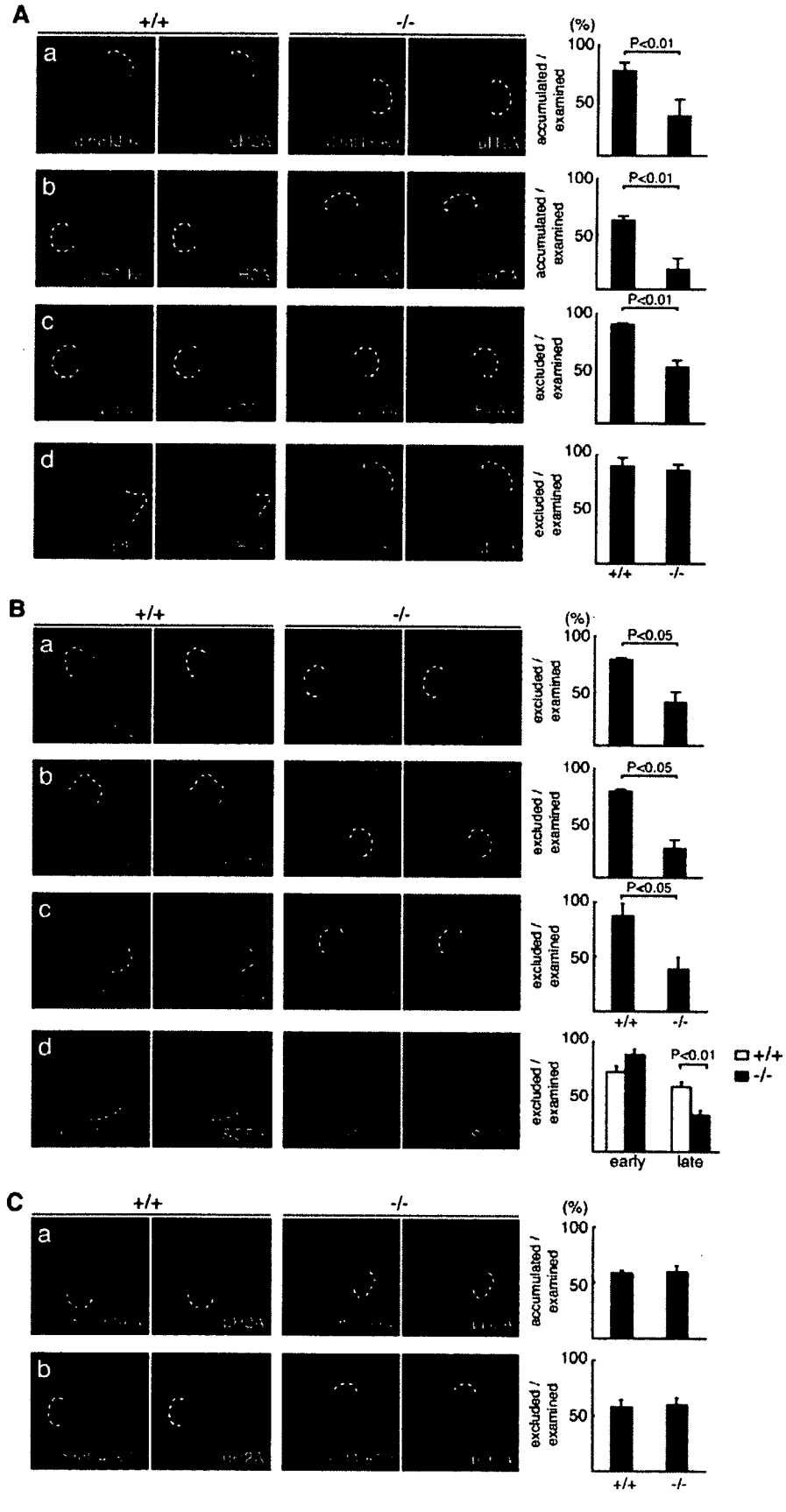

Fig. 5. Altered chromatin modifications at the XY body in *Scmh1*$^{+/-}$ spermatocytes.
(**A**) Immunostaining for dimethylated H3-K9, monomethylated H3-K9, phosphorylated RNA pol II, γH2A.X and uH2A in the spermatocyte spread. (**Aa**,**Ab**) Frequency of spermatocytes, in which dimethylated (a) or monomethylated (b) H3-K9 was enriched at the XY body demarcated by uH2A accumulation, was compared (left) and results were summarized (right). (**Ac**,**Ad**) Frequency of spermatocytes, in which phosphorylated RNA pol II (c) or acetylated H3-K9 (d) were excluded from the XY body, was compared (left) and results were summarized (right). (**Ba**,**Bb**) Frequency of spermatocytes, in which Phc1 (a) or Phc2 (b) were excluded from the XY body, was compared (left) and results were summarized (right). (**Bc**,**Bd**) Frequency of spermatocytes, in which trimethylated H3-K27 were excluded from the XY body was compared. Scp3 was used to substage the spermatocytes. (**C**) Frequency of spermatocytes, in which monomethylated H3-K4 (**Ca**) and dimethylated H4-K20 (**Cb**) were accumulated on the XY body, was compared (left) and results were summarized (right).

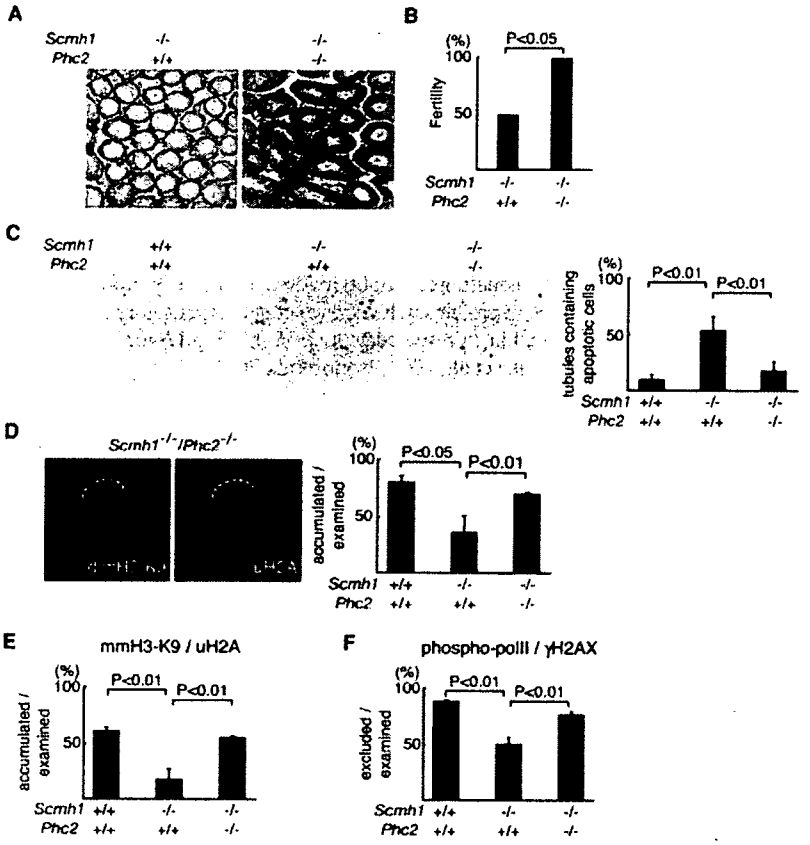

Fig. 6. Restoration of spermatogenic defects in *Scmh1*$^{-/-}$ testes by *Phc2* mutation.
(**A**) Restoration of morphological defects in *Scmh1*$^{-/-}$ testes by *Phc2* mutation. (**B**) Restoration of fertility in *Scmh1*$^{-/-}$;*Phc2*$^{-/-}$ mice. Results from ten mice with respective genotypes were summarized. (**C**) Significant reduction of apoptotic outbursts in *Scmh1*$^{-/-}$;*Phc2*$^{-/-}$ testes compared with *Scmh1*$^{-/-}$ single mutants. (Left) Incidence of apoptosis was examined in wild-type, *Scmh1*$^{-/-}$ and *Scmh1*$^{-/-}$;*Phc2*$^{-/-}$ testes at day 19 pp by TUNEL staining. (Right) Three hundred seminiferous tubules derived from five mice with respective genotypes were analyzed for the presence of TUNEL-positive cells and the results were summarized. (**D**) Restoration of spermatocytes, in which dimethylated H3-K9 was enriched at the XY body in *Scmh1*$^{-/-}$;*Phc2*$^{-/-}$ testes (left). Frequency of spermatocytes, in which dimethylated H3-K9 was accumulated on the XY body, was summarized (right). (**E**,**F**) Frequency of spermatocytes, in which monomethylated H3-K9 was enriched at (E) and phosphorylated pol II was excluded from (F) the XY body in *Scmh1*$^{-/-}$;*Phc2*$^{-/-}$ testes was compared.

and monomethylated H3-K9, the phosphorylated form of RNA pol II and Phc1 (Fig. 6D-F and Y.T., unpublished). Defects in spermatogenesis were also significantly alleviated in *Scmh1*$^{-/-}$*Phc2*$^{+/-}$ albeit to a lesser extent than dkos (Y.T., unpublished). Therefore *Phc2* mutation coincidentally restored aberrant chromatin modifications seen in the XY body of *Scmh1*$^{-/-}$ spermatocytes and their developmental arrest at the late pachytene stage. Taken together, this evidence suggests that Scmh1 is a regulatory component of Prc1 that mediates exclusion of Prc1 from the XY body at the pachytene stage of meiosis. It is likely that the lack of Phc2 components may accelerate this exclusion irrespective of Scmh1.

MSCI is not affected in *Scmh1*$^{-/-}$ spermatocytes

Transcriptional inactivation of sex chromosomes during spermatogenesis is accompanied by sequential changes in their histone modifications, which are notably affected in *Scmh1*$^{-/-}$ spermatocytes. We thus examined the degree of MSCI in *Scmh1*$^{-/-}$ testes, by performing genome-wide microarray-based analysis from three independent preparations of wild-type and *Scmh1*$^{-/-}$ spermatocytes at days 15, 18 and 20 pp and Cot1 RNA fluorescence in situ hybridization (FISH) (Fernandez-Capetillo et al., 2003; Turner et al., 2004; Turner et al., 2005). Average expression levels of genes located on the autosomes and sex chromosomes were compared between the wild type and *Scmh1*$^{-/-}$ after conventional normalization. No significant changes were found in the expression of autosomal and sex chromosomal genes in *Scmh1*$^{-/-}$ spermatocytes (see Fig. S5A in the supplementary material). Concordant with this result, the XY chromatin domain enriched in γH2A.X was negative for Cot-1 RNA in *Scmh1*$^{-/-}$ spermatocytes as well as the wild type (see Fig. S5B in the supplementary material). In conclusion, sequential chromatin modifications mediated by Scmh1 are not required to maintain MSCI.

DISCUSSION

In this study, we generated *Scmh1* mutant mice and identified Scmh1 as an indispensable component of Prc1, based on the axial homeosis and premature senescence of MEFs in the homozygous mutants. We have further identified the role of Scmh1 in mediating the survival of late pachytene spermatocytes. Apoptotic elimination of *Scmh1*$^{-/-}$ spermatocytes is accompanied by the preceding failure of several specific chromatin modifications at the XY body, whereas synapsis of homologous autosomes is not affected. Therefore, it is suggested that Scmh1 is involved in regulating the sequential changes in chromatin modifications at the XY chromatin domain of the pachytene spermatocytes but is not required to maintain MSCI. Restoration of defects in *Scmh1*$^{-/-}$ spermatocytes by *Phc2* mutation indicates that Scmh1 exerts its molecular functions via its interaction with Prc1. Therefore, for the first time, we have been able to indicate a functional involvement of Prc1 during the meiotic prophase of male germ cells and a regulatory role of Scmh1 for Prc1, which presumably involves sex chromosomes.

Based on the present observations, we postulate that Scmh1 could primarily promote the exclusion of Prc1 components from the XY body in the pachytene spermatocytes because Scmh1 itself is a functional component of Prc1. By contrast, failure to maintain exclusion of trimethylated H3-K27 and to undergo H3-K9 methylation at the XY body in *Scmh1*$^{-/-}$ spermatocytes may occur

secondarily to the failure to exclude Prc1 from the XY body. At many loci, epistatic engagement of Prc1 by Prc2 has been shown to be essential for the mediation of transcriptional repression (Lee et al., 2006; Boyer et al., 2006; Fujimura et al., 2006). Preceding exclusion of trimethylated H3-K27, which represents Prc2 actions, for Prc1 exclusion from the XY body, is consistent with epistatic roles of Prc2 for Prc1 at the XY body. Therefore, Scmh1 may affect H3-K27 trimethylation at the XY body through the Prc1-Prc2 engagement. It is noteworthy that H3-K27 trimethylation has been shown to be regulated by Prc1 at the XY body. This may imply that Prc1-Prc2 engagement is a reciprocal rather than epistatic process at the XY body. This possibility should be addressed by using conditional mutants for Prc2 components. We also hypothesize a functional correlation between Prc1 exclusion and H3-K9 methylations at the XY body because the indispensable H3-K9 methyltransferase complex, composed of G9a and GLP, is constitutively associated with E2F6 complexes, which share at least Rnf2 and Ring1 components with Prc1. Moreover, several components of respective complexes are structurally related to each other (Ogawa et al., 2002; Trimarchi et al., 2001). Intriguingly, although Prc1 components, apart from Rnf2, have been shown to be excluded from the XY body at late pachytene stage, components of E2F6 complexes including Rnf2, RYBP, HP1γ and G9a are retained (Y.T., K.I. and H.K., unpublished). The most attractive scenario would be that exclusion of Prc1 is a prerequisite for the functional manifestation of E2F6 complexes to mediate the hypermethylation of H3-K9 at the XY body. We thus propose that Scmh1-mediated exclusion of Prc1 from the XY body might be a prerequisite for maintaining appropriate chromatin structure to undergo subsequent sequential chromatin remodeling of the XY chromatin in pachytene spermatocytes.

We also suggest that sequential changes in chromatin modifications of the sex chromosomes in the pachytene spermatocytes might be monitored by some meiotic checkpoint mechanisms. This is supported by the temporal concurrence of Prc1 exclusion from the XY body and apoptotic depletion of meiotic spermatocytes, their coincidental restorations by *Phc2* mutation, and normal oogenesis and fertility in *Scmh1*$^{-/-}$ females (Y.T. and H.K., unpublished). In addition, defects in the XY body formations have been shown to correlate with apoptotic depletion of meiotic spermatocytes by studies using *H2A.X* and *Brca1* mutants, although developmental arrests occurred by early pachytene stage (Fernandez-Capetillo et al., 2003; Xu et al., 2003). However, this link has not been substantially demonstrated.

Although Scmh1 has been shown to act together with Prc1, the role of Scmh1 for Prc1 might be modified in a tissue- or locus-specific manner because spermatogenic defects by *Scmh1* mutation are restored by *Phc2* mutation, whereas premature senescence of MEFs is enhanced mutually by both mutations (Y.T. and H.K., unpublished). This is supported by an immunofluorescence study revealing the co-localization of Scmh1 with other class 2 PcG proteins in subnuclear speckles in U2OS cells, whereas in female trophoblastic stem (TS) cells it is excluded from the inactive X chromosome domain, which is intensely decorated by Rnf2, Phc2 and Rnf110 (see Fig. S6A,B in the supplementary material) (Plath et al., 2004; de Napoles et al., 2004). It may be possible to postulate some additional factors that modify the molecular functions or subnuclear localization of Scmh1. Indeed, most of the soluble pool of SCM in *Drosophila* embryos is not stably associated with Prc1, although SCM is capable of assembling with the Polyhomeotic protein by their respective SPM domains in the Polycomb core complex (Peterson et al., 2004). As the SPM domain is shared, not only by *polyhomeotic* homologs, but also by multiple paralogs of the *Drosophila Scm* gene, namely *Scml1*, *Scml2*, *Sfmbt*, *l(3)mbt3* and others in mammals, these structurally related gene products may potentially interact with Scmh1 and modulate its functions. Conservations of crucial amino acid residues required for the mutual interaction of SPM domains and multiple mbt repeats in these proteins may further suggest functional overlap with Scmh1. It is notable that phenotypic expressions of *Scmh1* mutation are quite variable during spermatogenesis and axial development even after more than five times backcrossing to a C57Bl/6 background. This incomplete penetrance might involve multiple paralogs of the canonical Scm proteins, which may act in compensatory manner for *Scmh1* mutation, as revealed between *Rnf110* and *Bmi1* or *Phc1* and *Phc2* (Akasaka et al., 2001; Isono et al., 2005).

We are grateful to Drs M. Vidal and W. Baarends for the critical reading of the manuscript. This project was supported by Special Coordination Funds for Promoting Science and Technology from the Ministry of Education, Culture, Sports, Science and Technology, the Japanese Government.

Supplementary material

Supplementary material for this article is available at http://dev.biologists.org/cgi/content/full/134/3/579/DC1

References

Akasaka, T., Kanno, M., Balling, R., Mieza, M. A., Taniguchi, M. and Koseki, H. (1996). A role for mel-18, a Polycomb group-related vertebrate gene, during the anteroposterior specification of the axial skeleton. *Development* **122**, 1513-1522.

Akasaka, T., van Lohuizen, M., van der Lugt, N., Mizutani-Koseki, Y., Kanno, M., Taniguchi, M., Vidal, M., Alkema, M., Berns, A. and Koseki, H. (2001). Mice doubly deficient for the Polycomb Group genes Mel18 and Bmi1 reveal synergy and requirement for maintenance but not initiation of Hox gene expression. *Development* **128**, 1587-1597.

Atsuta, T., Fujimura, S., Moriya, H., Vidal, M., Akasaka, T. and Koseki, H. (2001). Production of monoclonal antibodies against mammalian Ring1B proteins. *Hybridoma* **20**, 43-46.

Baarends, W. M., Hoogerbrugge, J. W., Roest, H. P., Ooms, M., Vreeburg, J., Hoeijmakers, J. H. and Grootegoed, J. A. (1999). Histone ubiquitination and chromatin remodeling in mouse spermatogenesis. *Dev. Biol.* **207**, 322-333.

Baarends, W. M., Wassenaar, E., van der Laan, R., Hoogerbrugge, J., Sleddens-Linkels, E., Hoeijmakers, J. H., de Boer, P. and Grootegoed, J. A. (2005). Silencing of unpaired chromatin and histone H2A ubiquitination in mammalian meiosis. *Mol. Cell. Biol.* **25**, 1041-1053.

Bel, S., Core, N., Djabali, M., Kieboom, K., Van der Lugt, N., Alkema, M. J. and Van Lohuizen, M. (1998). Genetic interactions and dosage effects of Polycomb group genes in mice. *Development* **125**, 3543-3551.

Bornemann, D., Miller, E. and Simon, J. (1996). The Drosophila Polycomb group gene Sex comb on midleg (Scm) encodes a zinc finger protein with similarity to polyhomeotic protein. *Development* **122**, 1621-1630.

Boyer, L. A., Plath, K., Zeitlinger, J., Brambrink, T., Mederios, L. A., Lee, T. I., Levine, S. S., Wernig, M., Tajonar, A., Ray, M. K. et al. (2006). Polycomb complexes repress developmental regulators in murine embryonic stem cells. *Nature* **441**, 349-353.

Cao, R., Wang, L., Xia, L., Erdjument-Bromage, H., Tempst, P. and Zhang, Y. (2002). Role of histone H3 lysine 27 methylation in Polycomb-group silencing. *Science* **298**, 1039-1043.

Celeste, A., Petersen, S., Romanienko, P. J., Fernandez-Capetillo, O., Chen, H. T., Sedelnikova, O. A., Reina-San-Martin, B., Coppola, V., Meffre, E., Difilippantonio, M. J. et al. (2002). Genomic instability in mice lacking histone H2AX. *Science* **296**, 922-927.

Cohen, P. E. and Pollard, J. W. (2001). Regulation of meiotic recombination and prophase I progression in mammals. *BioEssays* **23**, 996-1009.

de Napoles, M., Mermoud, J. E., Wakao, R., Tang, Y. A., Endoh, M., Appanah, R., Nesterova, T. B., Silva, J., Otte, A. P., Vidal, M. et al. (2004). Polycomb group proteins Ring1A/B link ubiquitylation of histone H2A to heritable gene silencing and X inactivation. *Dev. Cell* **7**, 663-676.

Fernandez-Capetillo, O., Mahadevaiah, S. K., Celeste, A., Romanienko, P. J., Camerini-Otero, R. D., Bonner, W. M., Manova, K., Burgoyne, P. and Nussenzweig, A. (2003). H2AX is required for chromatin remodeling and inactivation of sex chromosomes in male mouse meiosis. *Dev. Cell* **4**, 497-508.

Foulkes, N. S., Mellstrom, B., Benusiglio, E. and Sassone-Corsi, P. (1992). Developmental switch of CREM function during spermatogenesis: from antagonist to activator. *Nature* **355**, 80-84.

Franke, A., DeCamillis, M., Zink, D., Cheng, N., Brock, H. W. and Paro, R.

(1992). Polycomb and polyhomeotic are constituents of a multimeric protein complex in chromatin of Drosophila melanogaster. *EMBO J.* **11**, 2941-2950.
Fujimura, Y., Isono, K., Vidal, M., Endoh, M., Kajita, H., Mizutani-Koseki, Y., Takihara, Y., Van Lohuizen, M., Otte, A. P., Jenuwein, T. et al. (2006). Distinct roles of Polycomb group gene products in transcriptionally repressed and active domains of *Hoxb8*. *Development* **133**, 2371-2381.
Fujiwara, Y., Komiya, T., Kawabata, H., Sato, M., Fujimoto, H., Furusawa, M. and Noce, T. (1994). Isolation of a DEAD-family protein gene that encodes a murine homolog of Drosophila vasa and its specific expression in germ cell lineage. *Proc. Natl. Acad. Sci. USA* **91**, 12258-12262.
Gebuhr, T. C., Bultman, S. J. and Magnuson, T. (2000). Pc-G/trx-G and the SWI/SNF connection: developmental gene regulation through chromatin remodeling. *Genesis* **26**, 189-197.
Habu, T., Taki, T., West, A., Nishimune, Y. and Morita, T. (1996). The mouse and human homologs of DMC1, the yeast meiosis-specific homologous recombination gene, have a common unique form of exon-skipped transcript in meiosis. *Nucleic Acids Res.* **24**, 470-477.
Hoyer-Fender, S., Costanzi, C. and Pehrson, J. R. (2000). Histone macroH2A1.2 is concentrated in the XY-body by the early pachytene stage of spermatogenesis. *Exp. Cell Res.* **258**, 254-260.
Isono, K., Fujimura, Y., Shinga, J., Yamaki, M. O., Wang, J., Takihara, Y., Murahashi, Y., Takada, Y., Mizutani-Koseki, Y. and Koseki, H. (2005). Mammalian polyhomeotic homologues Phc2 and Phc1 act in synergy to mediate polycomb repression of Hox genes. *Mol. Cell. Biol.* **25**, 6694-6706.
Jacobs, J. J., Kieboom, K., Marino, S., DePinho, R. A. and van Lohuizen, M. (1999). The oncogene and Polycomb-group gene bmi-1 regulates cell proliferation and senescence through the ink4a locus. *Nature* **397**, 164-168.
Jürgens, G. (1985). A group of genes controlling spatial expression of the bithorax complex in *Drosophila*. *Nature* **316**, 153-155.
Kamijo, T., Zindy, F., Roussel, M. F., Quelle, D. E., Downing, J. R., Ashmun, R. A., Grosveld, G. and Sherr, C. J. (1997). Tumor suppression at the mouse INK4a locus mediated by the alternative reading frame product p19ARF. *Cell* **91**, 649-659.
Kessel, M. and Gruss, P. (1991). Homeotic transformations of murine vertebrae and concomitant alteration of Hox codes induced by retinoic acid. *Cell* **67**, 89-104.
Khalil, A. M., Boyar, F. Z. and Driscoll, D. J. (2004). Dynamic histone modifications mark sex chromosome inactivation and reactivation during mammalian spermatogenesis. *Proc. Natl. Acad. Sci. USA* **101**, 16583-16587.
Kim, J., Daniel, J., Espejo, A., Lake, A., Krishna, M., Xia, L., Zhang, Y. and Bedford, M. T. (2006). Tudor, MBT and chromo domains gauge the degree of lysine methylation. *EMBO Rep.* **7**, 397-403.
Klink, A., Lee, M. and Cooke, H. J. (1997). The mouse synaptosomal complex protein gene Sycp3 maps to band C of chromosome 10. *Mamm. Genome* **8**, 376-377.
Klymenko, T., Papp, B., Fischle, W., Köcher, T., Schelder, M., Fritsch, C., Wild, B., Wilm, M. and Müller, J. (2006). A Polycomb group protein complex with sequence-specific DNA-binding and selective methyl-lysine-binding activities. *Genes Dev.* **20**, 1110-1122.
Kuzmichev, A., Nishioka, K., Erdjument-Bromage, H., Tempst, P. and Reinberg, D. (2002). Histone methyltransferase activity associated with a human multiprotein complex containing the Enhancer of Zeste protein. *Genes Dev.* **16**, 2893-2905.
Laible, G., Wolf, A., Dorn, R., Reuter, G., Nislow, C., Lebersorger, A., Popkin, D., Pillus, L. and Jenuwein, T. (1997). Mammalian homologues of the Polycomb-group gene Enhancer of zeste mediate gene silencing in Drosophila heterochromatin and at S. cerevisiae telomeres. *EMBO J.* **16**, 3219-3232.
Lee, T. I., Jenner, R. G., Boyer, L. A., Guenther, M. G., Levine, S. S., Kumar, R. M., Chevalier, B., Johnstone, S. E., Cole, M. F., Isono, K. et al. (2006). Control of developmental regulators by Polycomb in human embryonic stem cells. *Cell* **125**, 301-313.
Levine, S. S., Weiss, A., Erdjument-Bromage, H., Shao, Z., Tempst, P. and Kingston, R. E. (2002). The core of the polycomb repressive complex is compositionally and functionally conserved in flies and humans. *Mol. Cell. Biol.* **22**, 6070-6078.
Mahadevaiah, S. K., Turner, J. M., Baudat, F., Rogakou, E. P., de Boer, P., Blanco-Rodriguez, J., Jasin, M., Keeney, S., Bonner, W. M. and Burgoyne, P. S. (2001). Recombinational DNA double-strand breaks in mice precede synapsis. *Nat. Genet.* **27**, 271-276.
Mettus, R. V., Litvin, J., Wali, A., Toscani, A., Latham, K., Hatton, K. and Reddy, E. P. (1994). Murine A-myb: evidence for differential splicing and tissue-specific expression. *Oncogene* **9**, 3077-3086.
Miyagishima, H., Isono, K., Fujimura, Y., Iyo, Y., Takihara, Y., Masumoto, H., Vidal, M. and Koseki, H. (2003). Dissociation of mammalian Polycomb-group proteins, Ring1B and Rae28/Ph1, from the chromatin correlates with configuration changes of the chromatin in mitotic and meiotic prophase. *Histochem. Cell Biol.* **120**, 111-119.
Montini, E., Buchner, G., Spalluto, C., Andolfi, G., Caruso, A., den Dunnen, J. T., Trump, D., Rocchi, M., Ballabio, A. and Franco, B. (1999). Identification of SCML2, a second human gene homologous to the Drosophila sex comb on midleg (Scm): a new gene cluster on Xp22. *Genomics* **58**, 65-72.
Odorisio, T., Mahadevaiah, S. K., McCarrey, J. R. and Burgoyne, P. S. (1996). Transcriptional analysis of the candidate spermatogenesis gene Ube1y and of the closely related Ube1x shows that they are coexpressed in spermatogonia and spermatids but are repressed in pachytene spermatocytes. *Dev. Biol.* **180**, 336-343.
Ogawa, H., Ishiguro, K., Gaubatz, S., Livingston, D. M. and Nakatani, Y. (2002). A complex with chromatin modifiers that occupies E2F- and Myc-responsive genes in G0 cells. *Science* **296**, 1132-1136.
Paro, R. (1995). Propagating memory of transcriptional states. *Trends Genet.* **11**, 295-297.
Perry, J., Palmer, S., Gabriel, A. and Ashworth, A. (2001). A short pseudoautosomal region in laboratory mice. *Genome Res.* **11**, 1826-1832.
Peterson, A. J., Mallin, D. R., Francis, N. J., Ketel, C. S., Stamm, J., Voeller, R. K., Kingston, R. E. and Simon, J. A. (2004). Requirement for sex comb on midleg protein interactions in Drosophila polycomb group repression. *Genetics* **167**, 1225-1239.
Pirrotta, V. (1997). PcG complexes and chromatin silencing. *Curr. Opin. Genet. Dev.* **7**, 249-258.
Plath, K., Talbot, D., Hamer, K. M., Otte, A. P., Yang, T. P., Jaenisch, R. and Panning, B. (2004). Developmentally regulated alterations in Polycomb repressive complex 1 proteins on the inactive X chromosome. *J. Cell Biol.* **167**, 1025-1035.
Richler, C., Dhara, S. K. and Wahrman, J. (2000). Histone macroH2A1.2 is concentrated in the XY compartment of mammalian male meiotic nuclei. *Cytogenet. Cell Genet.* **89**, 118-120.
Scherthan, H., Jerratsch, M., Dhar, S., Wang Y. A., Goff, S. P. and Pandita T. K. (2000). Meiotic telomere distribution and Sertoli cell nuclear architecture are altered in Atm- and Atm-p53-deficient mice. *Mol. Cell Biol.* **20**, 7773-7783.
Schumacher, A., Faust, C. and Magnuson, T. (1996). Positional cloning of a global regulator of anterior-posterior patterning in mice. *Nature* **384**, 648.
Sewalt, R. G., van der Vlag, J., Gunster, M. J., Hamer, K. M., den Blaauwen, J. L., Satijn, D. P., Hendrix, T., van Driel, R. and Otte, A. P. (1998). Characterization of interactions between the mammalian polycomb-group proteins Enx1/EZH2 and EED suggests the existence of different mammalian polycomb-group protein complexes. *Mol. Cell. Biol.* **18**, 3586-3595.
Shao, Z., Raible, F., Mollaaghababa, R., Guyon, J. R., Wu, C. T., Bender, W. and Kingston, R. E. (1999). Stabilization of chromatin structure by PRC1, a Polycomb complex. *Cell* **98**, 37-46.
Singer-Sam, J., Robinson, M. O., Bellve, A. R., Simon, M. I. and Riggs, A. D. (1990). Measurement by quantitative PCR of changes in HPRT, PGK-1, PGK-2, APRT, MTase, and Zfy gene transcripts during mouse spermatogenesis. *Nucleic Acids Res.* **18**, 1255-1259.
Strahl, B. D. and Allis, C. D. (2000). The language of covalent histone modifications. *Nature* **403**, 41-45.
Sweeney, C., Murphy, M., Kubelka, M., Ravnik, S. E., Hawkins, C. F., Wolgemuth, D. J. and Carrington, M. (1996). A distinct cyclin A is expressed in germ cells in the mouse. *Development* **122**, 53-64.
Tanaka, S. S., Toyooka, Y., Akasu, R., Katoh-Fukui, Y., Nakahara, Y., Suzuki, R., Yokoyama, M. and Noce, T. (2000). The mouse homolog of Drosophila Vasa is required for the development of male germ cells. *Genes Dev.* **14**, 841-853.
Tomotsune, D., Takihara, Y., Berger, J., Duhl, D., Joo, S., Kyba, M., Shirai, M., Ohta, H., Matsuda, Y., Honda, B. M. et al. (1999). A novel member of murine Polycomb-group proteins, Sex comb on midleg homolog protein, is highly conserved, and interacts with RAE28/mph1 in vitro. *Differentiation* **65**, 229-239.
Trimarchi, J. M., Fairchild, B., Wen, J. and Lees, J. A. (2001). The E2F6 transcription factor is a component of the mammalian Bmi1-containing polycomb complex. *Proc. Natl. Acad. Sci. USA* **98**, 1519-1524.
Turner, J. M., Mahadevaiah, S. K., Benavente, R., Offenberg, H. H., Heyting, C. and Burgoyne, P. S. (2000). Analysis of male meiotic "sex body" proteins during XY female meiosis provides new insights into their functions. *Chromosoma* **109**, 426-432.
Turner, J. M., Burgoyne, P. S. and Singh, P. B. (2001). M31 and macroH2A1.2 colocalize at the pseudoautosomal region during mouse meiosis. *J. Cell Sci.* **114**, 3367-3375.
Turner, J. M., Aprelikova, O., Xu, X., Wang, R., Kim, S., Chandramouli, G. V., Barrett, J. C., Burgoyne, P. S. and Deng, C. X. (2004). BRCA1, histone H2AX phosphorylation, and male meiotic sex chromosome inactivation. *Curr. Biol.* **14**, 2135-2142.
Turner, J. M., Mahadevaiah, S. K., Fernandez-Capetillo, O., Nussenzweig, A., Xu, X., Deng, C. X. and Burgoyne, P. S. (2005). Silencing of unsynapsed meiotic chromosomes in the mouse. *Nat. Genet.* **37**, 41-47.
Usui, H., Ichikawa, T., Kobayashi, K. and Kumanishi, T. (2000). Cloning of a novel murine gene Sfmbt, Scm-related gene containing four mbt domains, structurally belonging to the Polycomb group of genes. *Gene* **248**, 127-135.
van de Vosse, E., Walpole, S. M., Nicolaou, A., van der Bent, P., Cahn, A., Vaudin, M., Ross, M. T., Durham, J., Pavitt, R., Wilkinson, J. et al. (1998). Characterization of SCML1, a new gene in Xp22, with homology to developmental polycomb genes. *Genomics* **49**, 96-102.

van der Vlag, J. and Otte, A. P. (1999). Transcriptional repression mediated by the human polycomb-group protein EED involves histone deacetylation. *Nat. Genet.* **23**, 474-478.

van Lohuizen, M., Tijms, M., Voncken, J. W., Schumacher, A., Magnuson, T. and Wientjens, E. (1998). Interaction of mouse polycomb-group (Pc-G) proteins Enx1 and Enx2 with Eed: indication for separate Pc-G complexes. *Mol. Cell. Biol.* **18**, 3572-3579.

Wang, H., Wang, L., Erdjument-Bromage, H., Vidal, M., Tempst, P., Jones, R. S. and Zhang, Y. (2004). Role of histone H2A ubiquitination in Polycomb silencing. *Nature* **431**, 873-878.

Watanabe, D., Yamada, K., Nishina, Y., Tajima, Y., Koshimizu, U., Nagata, A. and Nishimune, Y. (1994). Molecular cloning of a novel Ca(2+)-binding protein (calmegin) specifically expressed during male meiotic germ cell development. *J. Biol. Chem.* **269**, 7744-7749.

Xu, X., Aprelikova, O., Moens, P., Deng, C. X. and Furth, P. A. (2003). Impaired meiotic DNA-damage repair and lack of crossing-over during spermatogenesis in BRCA1 full-length isoform deficient mice. *Development* **130**, 2001-2012.

Yuasa, S. (1996). Bergmann glial development in the mouse cerebellum as revealed by tenascin expression. *Anat. Embryol.* **194**, 223-234.

Zhao, G. Q. and Hogan, B. L. (1996). Evidence that mouse Bmp8a (Op2) and Bmp8b are duplicated genes that play a role in spermatogenesis and placental development. *Mech. Dev.* **57**, 159-168.

Molecular Cell
Article

A Phosphorylated Form of Mel-18 Targets the Ring1B Histone H2A Ubiquitin Ligase to Chromatin

Sarah Elderkin,[1] Goedele N. Maertens,[3] Mitsuhiro Endoh,[4] Donna L. Mallery,[2] Nick Morrice,[5] Haruhiko Koseki,[4] Gordon Peters,[3] Neil Brockdorff,[1,6,*] and Kevin Hiom[2,6,*]
[1]Medical Research Council Clinical Sciences Centre, Faculty of Medicine, Imperial College London, Hammersmith Hospital Campus, Du Cane Road, London W12 ONN, UK
[2]Medical Research Council Laboratory of Molecular Biology, Hills Road, Cambridge CB2 2QH, UK
[3]Cancer Research UK, London Research Institute, 44 Lincolns Inn Fields, London WC2A 3PX, UK
[4]Department of Developmental Genetics, RIKEN Research Centre for Allergy and Immunology, RIKEN Yokohama Institute, 1-7-22 Suehiro, Tsutumi-Ku, Yokohama 230-0045, Japan
[5]MRC Protein Phosphorylation Unit, Sir James Black Centre, University of Dundee, Dundee DD1 5EH, Scotland, UK
[6]These authors contributed equally to this work.
*Correspondence: hiom@mrc-lmb.cam.ac.uk (K.H.), neil.brockdorff@csc.mrc.ac.uk (N.B.)
DOI 10.1016/j.molcel.2007.08.009

SUMMARY

Recent studies have shown that PRC1-like Polycomb repressor complexes monoubiquitylate chromatin on histone H2A at lysine residue 119. Here we have analyzed the function of the polycomb protein Mel-18. Using affinity-tagged human MEL-18, we identify a polycomb-like complex, melPRC1, containing the core PRC1 proteins, RING1/2, HPH2, and CBX8. We show that, in ES cells, melPRC1 can functionally substitute for other PRC1-like complexes in *Hox* gene repression. A reconstituted subcomplex containing only Ring1B and Mel-18 functions as an efficient ubiquitin E3 ligase. This complex ubiquitylates free histone substrates nonspecifically but is highly specific for histone H2A lysine 119 in the context of nucleosomes. Mutational analysis demonstrates that while Ring1B is required for E3 function, Mel-18 directs this activity to H2A lysine 119 in chromatin. Moreover, this substrate-targeting function of Mel-18 is dependent on its prior phosphorylation at multiple residues, providing a direct link between chromatin modification and cell signaling pathways.

INTRODUCTION

Polycomb group (PcG) repressor proteins were originally identified as factors involved in the maintenance of homeobox gene silencing during development in *D. melanogaster*. Further studies showed these factors to be conserved in a wide range of organisms, with key roles in developmental gene regulation, cell-cycle regulation, and pluripotency in embryonic stem (ES) cells (for recent reviews, see Jorgensen et al., 2006; Schwartz and Pirrotta, 2007).

Biochemical and genetic studies revealed that PcG proteins are components of at least two major multiprotein complexes, termed *p*olycomb *r*epressor complex 1 (PRC1) (Saurin et al., 2001; Shao et al., 1999) and PRC2 (Cao et al., 2002; Czermin et al., 2002; Kuzmichev et al., 2002; Muller et al., 2002). Other PcG complexes have also been described (Klymenko et al., 2006; Kuzmichev et al., 2004). Analyses of PRC1 in *D. melanogaster* (Shao et al., 1999), and subsequently in mammalian cells (Levine et al., 2002), defined the core components Polycomb (PC), posterior sex combs (PSC), polyhomeotic (PH), and RING1 (dRING). There are two or more homologs of each of these core proteins in human and other higher organisms. It remains to be determined whether these homologs have equivalent and/or unique functions.

Early studies demonstrated that purified and reconstituted PRC1 complexes can inhibit transcription and SWI/SNF-mediated chromatin remodeling (Francis et al., 2001; Shao et al., 1999). More recently, PRC1-like complexes, containing the core components RING1/2 and BMI1, were isolated from HeLa cells and shown to function as a ubiquitin E3 ligase that specifically monoubiquitylates histone H2A lysine 119, this activity being attributed to the RING2 (Ring1B) protein (Wang et al., 2004). Monoubiquitylated H2A (H2Aub1) is a relatively abundant histone modification, estimated to comprise 5%–15% of available nucleosomal H2A (West and Bonner, 1980). Genetic studies revealed that mouse cells deleted for Ring1B and the closely related homolog Ring1A, exhibit global loss of H2Aub1 (de Napoles et al., 2004).

Although the function of H2Aub1 remains to be determined, several pieces of evidence suggest that it is important for PRC1-mediated gene repression. First, PRC1 targets, such as *Hox* genes and the inactive X chromosome in mammals, are enriched for H2Aub1 (Cao et al., 2005;

de Napoles et al., 2004). Second, in *D. melanogaster*, a point mutation affecting only the RING finger domain of dRING results in a classical polycomb phenotype (Fritsch et al., 2003). Analysis of this mutant protein in vitro demonstrated concomitant loss of H2A E3 ubiquitin ligase activity (Wang et al., 2004).

While, in vitro, the histone ubiquitin ligase activity of mouse Ring1B can be stimulated by other subunits of PRC1 (Cao et al., 2005), subcomplexes containing either human RING1 (Ring1A) or RING2 (Ring1B) with BMI1 exhibited E3 activity equivalent to that of PRC1 purified from HeLa cells (Wei et al., 2006). Since addition of other PRC1 proteins to this latter subcomplex did not enhance its E3 activity, it is likely that the Ring1B/Bmi1 subcomplex comprises a minimal bipartite ubiquitin E3 ligase. Similar synergistic effects have been reported for the RING finger proteins Brca1 and Bard1, in which heterodimerization markedly stimulates the E3 ubiquitin ligase activity of Brca1 (Hashizume et al., 2001; Mallery et al., 2002). Furthermore, like Brca1/Bard1, the ubiquitin ligase function of Ring1B/Bmi1 is enhanced by autoubiquitylation (Ben-Saadon et al., 2006; Chen et al., 2002; Hashizume et al., 2001; Mallery et al., 2002).

Structural analysis of a Ring1B/Bmi1 complex (Buchwald et al., 2006; Li et al., 2006) revealed extensive interactions between the RING finger domains of Ring1B and Bmi1 and that the association with the ubiquitin-conjugating enzyme (E2) maps to a surface on Ring1B (Buchwald et al., 2006). Although Bmi1 is not required for E2 interaction, it has been shown to contribute to the stabilization of the PRC1 complex (Cao et al., 2005; Wei et al., 2006).

In mammals, there are at least four paralogs of the *D. melanogaster* RING finger protein PSC: Bmi1, Mel-18, MBLR, and NSPc1 (Akasaka et al., 2002; Brunk et al., 1991; van Lohuizen et al., 1991). Evidence suggests that these paralogs may interact with other PcG proteins to form a set of distinct but related complexes. Specifically, MBLR together with Ring1B is implicated in the E2F6 complex (Ogawa et al., 2002), and NSPc1 together with Ring1B and other PRC1 proteins is a component of a BCOR corepressor complex (Gearhart et al., 2006).

Mel-18 protein is 70% identical to Bmi1 at the amino acid level. Genetic experiments suggest that these proteins may have similar or overlapping functions. Mel-18 knockout mice exhibit homeotic transformations and cell-cycle deficiencies similar to those reported for Bmi1 mutants (Akasaka et al., 1996, 1997, 2001; van der Lugt et al., 1994), and the Mel-18 protein localizes to PRC1 target genes (Fujimura et al., 2006). Despite this, Mel-18 has not been identified in purified PRC1 or related complexes (Gearhart et al., 2006; Levine et al., 2002; Ogawa et al., 2002; Wang et al., 2004) and, unlike Bmi1, did not enhance the E3 ligase activity of Ring1B in vitro (Cao et al., 2005).

In this study, we investigated the function of this protein and whether it forms part of a functional polycomb repressive complex. We show that Mel-18 is indeed a component of a PRC1-like complex and that it can functionally substitute for Bmi1 in repressing *Hox* gene expression in ES cells. Furthermore, contrary to previous reports, we show that a holocomplex and a reconstituted Ring1B/Mel-18 subcomplex efficiently ubiquitylate H2A lysine 119. Interestingly, we find that a phosphorylated form of Mel-18 is important for targeting this complex to histone H2A lysine 119. Our results provide insights into the mechanism of action of H2A ubiquitin E3 ligase complexes and demonstrate a direct link between chromatin regulation by PcG repressor complexes and cell signaling pathways.

RESULTS

Affinity Purification of a Polycomb-like Complex

To investigate whether, like other polycomb proteins, MEL-18 is present in cells as part of a large multiprotein complex, we expressed and purified human MEL-18 protein, fused to a tandem affinity purification (TAP) tag, from 293T cells. Mass spectrometry analysis identified several proteins that copurify with MEL-18 (Figure 1A). These proteins, namely RING1/2, the short isoform of HPH2a (Yamaki et al., 2002; Tonkin et al., 2002), and CBX8, were previously identified as core PRC1 components (Shao et al., 1999; Levine et al., 2002). Other paralogs of HPH2 were present in substoichiometric amounts, suggesting that multiple MEL-18 complexes might exist in the cell. Importantly, the MEL-18 paralog BMI1 was not present in this complex, and, conversely, MEL-18 was not present in a PRC1-like complex isolated using TAP-tagged BMI1 (see Figure S1 in the Supplemental Data available with this article online). Thus, MEL-18 and BMI1 proteins are components of similar but mutually exclusive PRC1-like complexes. We subsequently refer to these complexes as MEL-18 PRC1 (melPRC1) and BMI1 PRC1 (bmiPRC1).

melPRC1 is also present in mouse ES cells. Nickel-affinity purification of Mel18-FlagHis expressed in BM3 ES cells, which lack endogenously expressed Mel-18 and Bmi1, also "pulled down" Ring1A, Ring1B, and mPh1, homologs of the human PRC1 proteins RING1/2 and HPH1 (Figures S2A and S2B). Copurification of mPh1, rather than mPh2, most likely reflects low levels of mPh2 expression in mouse ES cells (H.K. and M.E., unpublished data).

Regulation of *Hox* Gene Expression in Embryonic Stem Cells

Microarray-based gene expression profiles identified several *Hox* genes whose expression is upregulated in cells lacking Mel-18 and Bmi1 (H.K. and M.E., unpublished data). Using RT-PCR, we measured expression of several of these genes in independently derived clones of BM3 that overexpress Mel-18-FlagHis (BM3-1, BM3-2, and BM3-3). In these cells, expression of the *Hoxa1*, *Hoxa5*, *Hoxd4*, and *Hoxd8* genes was approximately 5- to 10-fold lower than in the parental BM3 cell line (Figure 1B). Downregulation of gene expression was not a general phenomenon, as expression

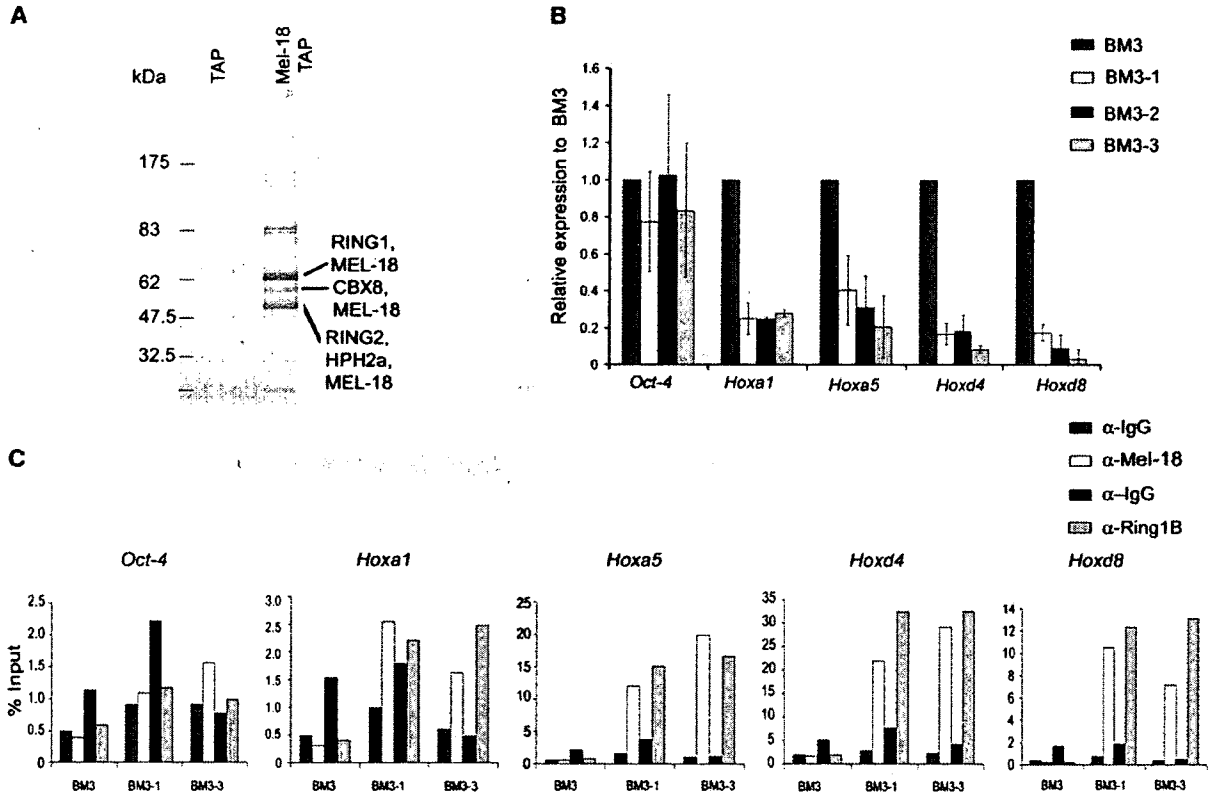

Figure 1. Mel-18 Forms a PRC1-like Complex that Represses *Hox* Gene Expression

(A) MEL-18 complex purified from 293T cells by TAP. Coomassie-stained gel showing proteins identified by mass spectrometry. Lane 1, proteins isolated by expression and purification of TAP alone, negative control. Lane 2, proteins isolated by expression and purification of TAP-Mel-18.

(B) Expression of *Hox* genes is downregulated in BM3 cells expressing Mel-18. Expression of *Hox* genes was analyzed by real-time RT-PCR in BM3 or BM3-1, BM3-2, and BM3-3, which express Mel-18-FlagHis. Gene expression levels were normalized against the average of two housekeeping genes (*GAPDH* and *HMBS*) and are represented as a ratio of expression in the parental cell line BM3. Expression of the *Oct-4*, *Hoxa1*, *Hoxa5*, *Hoxd4*, and *Hoxd8* genes is shown. Error bars represent the average standard deviation of five independent experiments.

(C) Mel-18 localizes to the promoter of *Hox* genes. ChIP was performed using antibodies against either Mel-18 or Ring1B at the promoter regions of *Oct-4*, *Hoxa1*, *Hoxa5*, *Hoxd4*, and *Hoxd8* in BM3-1 and BM3-3 cells. Antibody against IgG was used as a control. Enrichment is represented as a percentage of input. Replicate experiments are shown in Figure S3.

of the *Oct-4* gene in the same cells was unaffected by Mel-18. Therefore, like PRC1, melPRC1 may function as a negative regulator of *Hox* gene expression in ES cells.

Localization of melPRC1 to *Hox* Gene Promoters

To determine whether melPRC1 localizes to the promoters of *Hox* genes, we performed chromatin immunoprecipitation (ChIP) analysis. As expected, neither Mel-18 nor Ring1B was enriched at the promoters of *Hox* genes or *Oct-4* in parental BM3 cells (Figure 1C and Figure S3). However, in BM3-1 and BM3-3 cells, we observed enrichment of both Ring1B and Mel-18 at the promoters of *Hoxa1*, *Hoxa5*, *Hoxd4*, and *Hoxd8*, but not at *Oct-4* (Figure 1C and Figure S3). Hence, there is a clear correlation between the repression of gene expression and the recruitment of melPRC1 to the promoters of *Hoxa1*, *Hoxa5*, *Hoxd4*, and *Hoxd8*.

Ring1B/Mel-18 Complex Is a Ubiquitin E3 Ligase

Although Bmi1 and Ring1B interact to form a ubiquitin ligase complex that ubiquitylates nucleosomes in vitro, no such activity has been reported for Mel-18. We expressed and purified recombinant Mel-18 and Ring1B proteins in a complex, from Sf9 cells (Figures 2A and 2C). We noted that while Ring1B migrates as a single species, Mel-18 migrates as several distinct bands after polyacrylamide gel electrophoresis (Figure 2A). Subsequent analysis revealed these bands to be different phosphorylated forms of Mel-18 (see below).

Contrary to a previous report (Cao et al., 2005), we found that Ring1B/Mel-18, in the presence of the ubiquitin-conjugating enzyme (E2) UbcH5C, efficiently monoubiquitylates nucleosomes in vitro (Figure 2B). Like many other RING domain E3 ligases, Ring1B/Mel-18 also undergoes autopolyubiquitylation (Figure 2B), mainly on Ring1B (data not shown).

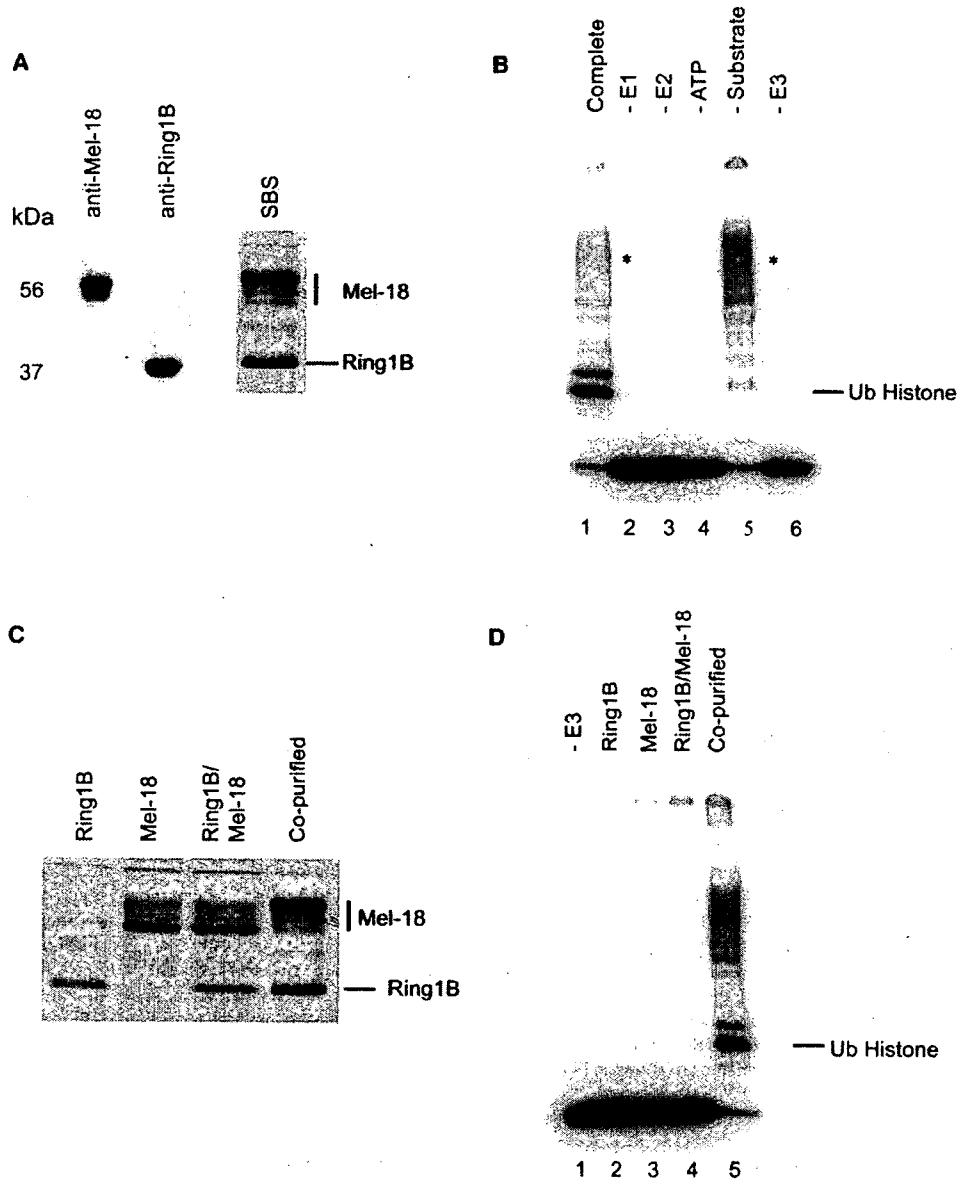

Figure 2. Ring1B/Mel-18 Complex Ubiquitylates Nucleosomes In Vitro

(A) FlagHis-tagged Ring1B and HA-tagged Mel-18 proteins were coexpressed and copurified from Sf9 cells as described in the Experimental Procedures. A 10 μl aliquot of the purified complex was analyzed by 12% SDS-PAGE and protein visualized by western blot using anti-Mel-18, anti-Ring1B antibodies (as indicated) or by staining with Simply Blue Safe Stain (Invitrogen) (SBS). Molecular weights are indicated.

(B) Ring1B/Mel-18-dependent ubiquitylation of chromatin requires ATP, E1, and E2 enzymes. Ubiquitylation assays were carried out as described in the Experimental Procedures with individual components omitted where indicated (lanes 2–6). The complete reaction is shown in lane 1. Ubiquitylated histone product is labeled. Autoubiquitylated Ring1B/Mel-18 complex is indicated by an asterix.

(C) Ring1B and Mel-18 were expressed and purified individually or as a complex from Sf9 cells. Proteins were visualized by staining with SBS. Shown are Ring1B alone (lane 1), Mel-18 alone (lane 2), Ring1B and Mel-18 mixed in vitro (lane 3), and copurified Ring1B/Mel-18 complex (lane 4).

(D) A complex of Mel-18 and Ring1B is required for efficient ubiquitylation of nucleosomes. Ubiquitylation assays were performed using the protein preparations described in the left panel.

We observed efficient ubiquitylation of nucleosomes only when Mel-18 and Ring1B were coexpressed and copurified as a complex (Figure 2D, lane 5). Neither Mel-18 or Ring1B purified individually nor a mixture of the two proteins exhibited strong E3 ligase activity (Figure 2D). This suggests, first, that both Mel-18 and Ring1B are required for the efficient ubiquitylation of nucleosomes and, second, that a factor (or factors)

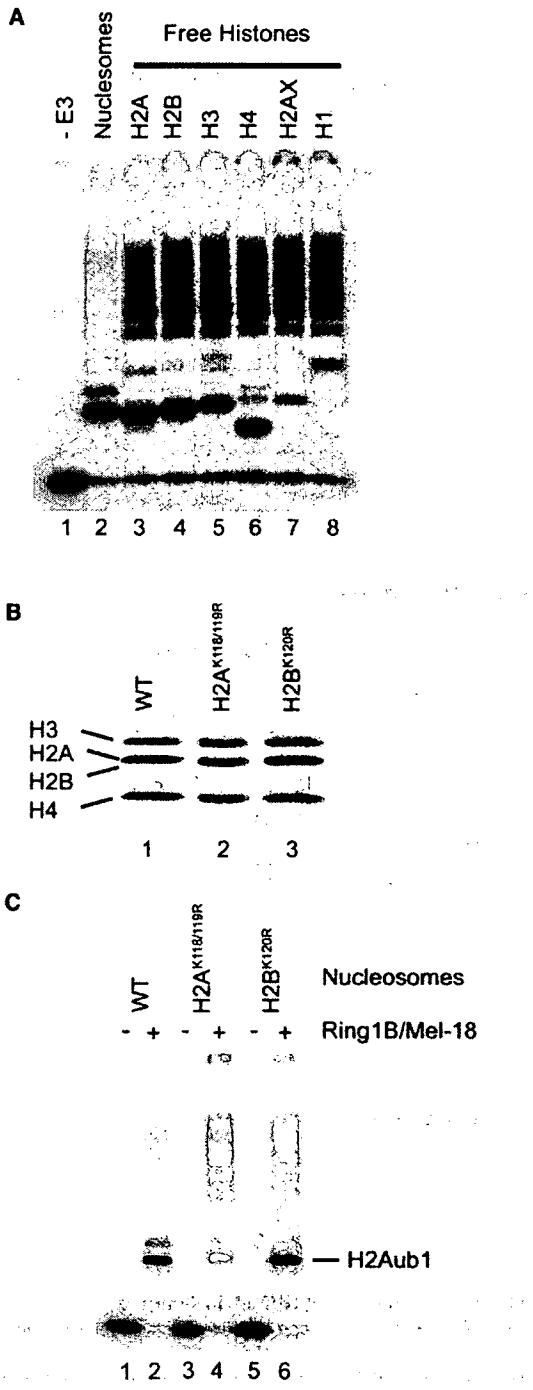

Figure 3. Ring1B/Mel-18 Complex Exhibits Defined Substrate Specificity

(A) Ubiquitylation assays were performed using 1 μg Ring1B/Mel-18 complex with various substrates, as indicated. Shown are 1.5 μg nucleosomes (lane 2); 1 μg of individual histones H2A, H2B, H3, and H4 (lanes 3–6); H2AX (lane 7); and H1 (lane 8). I^{125}-labeled products are shown.

(B) Purified reconstituted nucleosomes. Shown are wild-type nucleosome (lane 1), mutant $H2A^{K118/119R}$ nucleosome (lane 2), and mutant $H2B^{K120R}$ nucleosome (lane 3).

present during the assembly of the Ring1B/Mel-18 complex in Sf9 cells plays an important role in activating the ubiquitin ligase function of the complex (see below).

Ring1B/Mel-18 Ubiquitylates Histone H2A

In vitro, Ring1B/Mel-18 seemed to ubiquitylate nucleosomes on a single histone (Figure 3A, lane 2). Modification was largely monoubiquitylation, although some diubiquitylated histone was also observed. We next investigated ubiquitylation of individual histones in vitro. We found that, whereas Ring1B/Mel-18 ubiquitylates individual nucleosome core histones with similar high efficiency, ubiquitylation of H1, the linker histone, was much less efficient (Figure 3A, lanes 3–8, respectively). Hence it appears that the Ring1B/Mel-18 complex acquires specificity for its histone substrate only in a nucleosomal context.

SDS-PAGE suggested that ubiquitylation of nucleosomes occurred on either histone H2A (H2Aub1) or histone H2B (H2Bub1). To investigate which of these histones is modified by Ring1B/Mel-18, we made nucleosomes with recombinant histone proteins in which either lysine 118 and 119 of H2A or lysine 120 of H2B were substituted with arginine residues (Figure 3B, lanes 2 and 3, respectively). We found that, whereas the Ring1B/Mel-18 ubiquitylated wild-type nucleosomes and those containing $H2B^{K120R}$ mutant with equal efficiency (Figure 3C, lanes 1 and 2 and 5 and 6, respectively), those made with $H2A^{K118/119R}$ were largely unmodified (Figure 3C, lanes 3 and 4).

Comparison of Mel-18/Ring1B with Bmi-1/Ring1B revealed that these complexes exhibit similar specific activity toward H2A on a nucleosomal substrate (Figure S4A). This was also the case when we compared the activity of melPRC1 and bmiPRC1 holocomplexes isolated from 293T cells (Figure S4B). We conclude that Ring1B/Mel-18 is a chromatin E3 ubiquitin ligase with specificity for lysines 118 or 119 of histone H2A. Again, this mirrors the specificity of the bmiPRC1 ubiquitin ligase and, because H2Aub1 is thought to be a repressive modification, is in keeping with the role of melPRC1 as a negative regulator of gene expression.

The Role of the Ring1B RING Domain in Ubiquitylation

RING domains are known to confer E3 ligase function. To investigate the role of the Ring1B RING domain in ubiquitylation of H2A, we made cysteine-to-glycine substitutions at residue 87 or 90, representing cysteines 7 and 8 of the RING domain (Figure 4A). We also made mutant protein with an isoleucine-to-alanine substitution at residue 53, which is critical for interactions with the

(C) Ubiquitylation of reconstituted nucleosomes by Ring1B/Mel-18 in vitro. Wild-type nucleosomes (lanes 1 and 2), histone $H2A^{K118/119R}$ mutant (lanes 3 and 4), and histone $H2B^{K120R}$ mutant (lanes 5 and 6) nucleosomes are shown.

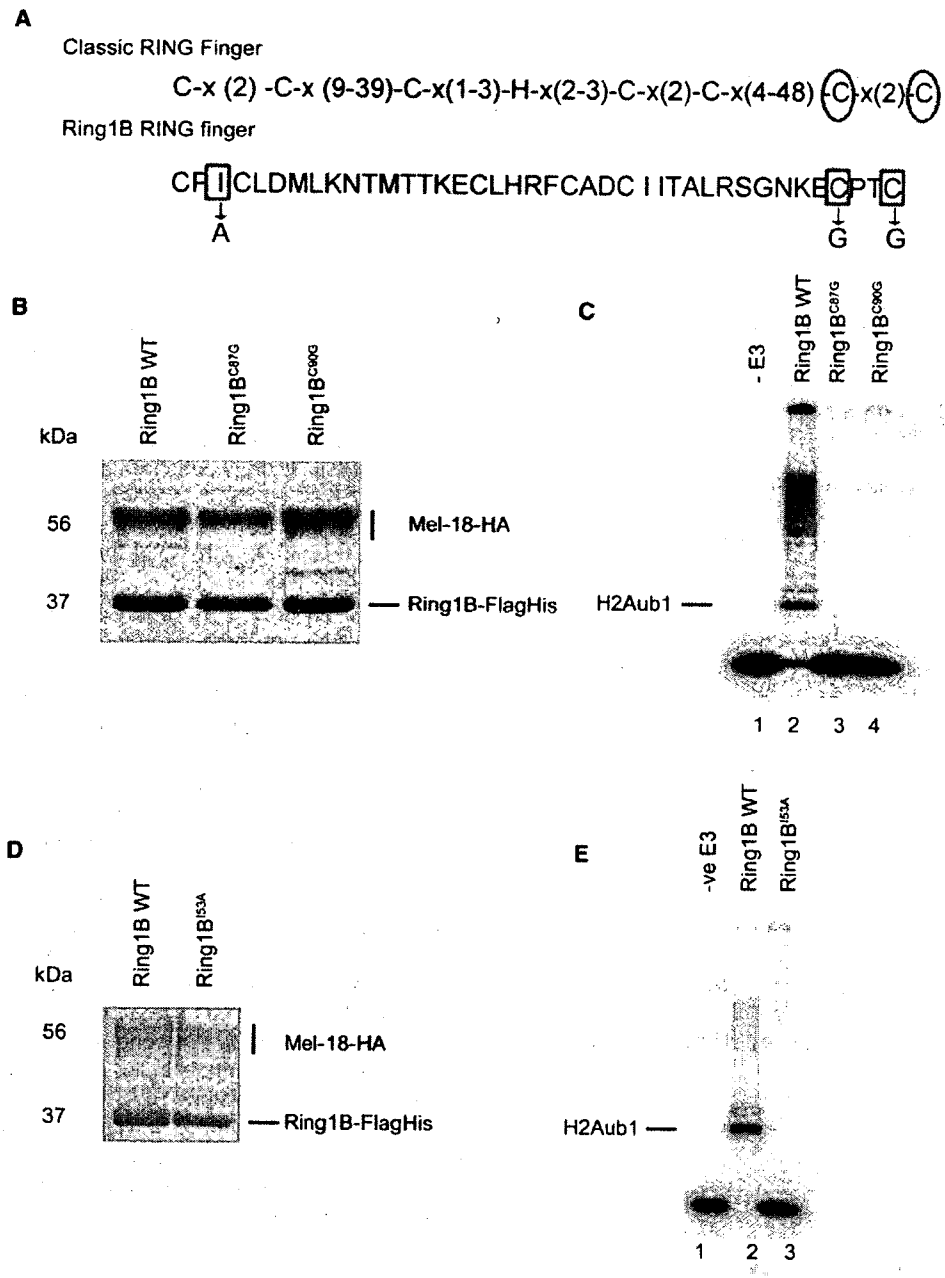

Figure 4. Mutations in the RING Domain of Ring1B Abolish the E3 Ligase Activity of the Ring1B/Mel-18 Complex

(A) Amino acid sequence of a consensus RING domain and the RING domain of Ring1B. Boxed residues represent the substituted amino acids and correspond to the circled residues of the consensus RING domain.

(B) Wild-type and mutant Ring1B/Mel-18 complexes. Wild-type, Ring1B^{C87G}/Mel-18, and Ring1B^{C90G}/Mel-18 complexes are shown. Molecular weight markers are indicated.

(C) Ring1B^{C87G}/Mel-18 and Ring1B^{C90G}/Mel-18 complexes were examined for E3 ligase activity in vitro. I^{125}-ubiquitylated histone H2A (H2Aub1) product is indicated.

(D) Wild-type and mutant Ring1B^{I53A}/Mel-18 complex.

(E) Mutant Ring1B^{I53A}/Mel-18 complex was examined for E3 ligase activity. Ubiquitylated H2A (H2Aub1) product is indicated.

ubiquitin-conjugating enzyme Ubc5C in other E3 ligases (Brzovic et al., 2003) (Figure 4A). Although these mutant proteins copurified normally with Mel-18 (Figures 4B and 4D), they were defective for the ubiquitylation of the nucleosome substrate and for autoubiquitylation (Figures 4C and 4E). In addition, these mutants were unable to ubiquitylate free histones (data not shown). We infer that the RING domain of Ring1B plays a central role in conferring

E3 ligase activity to the Ring1B/Mel-18 complex, and this most likely involves the recruitment of the ubiquitin-charged E2 to the complex.

Mel-18 RING Domain Is Important for Recognition of the Nucleosome

We also made mutant proteins with cysteine-to-glycine substitutions at residues 53 and 56 in the RING domain of Mel-18 (Figure 5A). These mutants also copurified normally in a complex with Ring1B (Figure 5B). However, while Ring1B/Mel-18^{C56G} ubiquitylated nucleosomes with normal efficiency (Figure 5C, lanes 2 and 4), Ring1B/Mel-18^{C53G} did not (Figure 5C, lane 3). Nevertheless, Ring1B/Mel-18^{C53G} was not completely defective, as it retained autoubiquitylation activity and the ability to ubiquitylate free histones (Figure 5C, lane 3, and Figure 5D, lanes 3–8). Therefore, in contrast to Ring1B, the RING domain of Mel-18 is not required for E3 function per se but may function specifically to mediate the interaction with its chromatin substrate.

Phosphorylation of Mel-18

Both Mel-18 purified from ES cells as well as recombinant Mel-18 migrate as several distinct bands after SDS-PAGE (Figures 6A and 6B, respectively). These are different phosophorylated forms of Mel-18, most of which disappear upon treatment with alkaline phosphatase (AP) (Figures 6A and 6B). Interestingly, in HeLa cells, the phosphorylated form of MEL-18 is associated with the chromatin fraction (Figure S5) and remains so throughout the cell cycle (Figure S6). We note that the forms of MEL-18 that are phosphorylated to a lesser extent are no longer associated with chromatin during mitosis (Figure S6B). However, it is unclear whether this represents redistribution or degradation of hypophosphorylated MEL-18.

The phosphorylated recombinant Mel-18 protein was subjected to tryptic digest and mass spectrometry. LC-MS/MS analysis led to the positive identification of two phosphopeptides where Ser132 was phosphorylated in one (minor site) and Ser254, Ser260, and Ser265 were phosphorylated in the second (Table S1). Additionally, MALDI-TOF mass spectrometry identified phosphopeptides encompassing residues 263–329 (+1–3 PO_4) and 236–329 (+2–8 PO_4) (data not shown). This was validated by inspecting the survey scans from the LTQ Orbitrap. The same peptides were observed in high charge states (5+ to 10+) at high mass accuracy (data not shown). The resultant LC-MS/MS spectra from these ions did not yield sufficiently rich fragmentation data to assign phosphorylation sites. However, after elastase digestion of a tryptic digest of Mel-18, shorter overlapping fragments of the same region of the protein were generated, and the resultant spectra permitted the assignment of phosphorylation sites at Ser110, Ser254, Ser258, Ser260, Ser265, Ser278, Thr281, Ser286, and Ser299 (Table S1). These data resolved the orbitrap survey scan result, which detected a tryptic peptide encompassing residues 236–329 with up to eight phosphorylation sites.

The location of phosphorylation sites is summarized in Figure 7A. The majority cluster in the proline/serine-rich domain at the C terminus with two sites, one of which is relatively weak, present in the central domain of the protein. Phosphorylated residues are conserved in human and mouse Mel-18 (Figure S7A), and all of the sites except Ser254 and Ser299 are also conserved in Bmi1 (Figure S7B).

Phosphorylation of Mel-18 Is Required for Ubiquitylation of Nucleosomes

We noted that both wild-type Mel-18, purified independently of Ring1B, and the Mel-18^{C53G} mutant protein exist largely in the nonphosphorylated form (Figures 2B and 5B). Since neither of these protein complexes is able to ubiquitylate nucleosomes in vitro, we reasoned that there might be a correlation between the ubiquitin ligase function of Mel-18 and its phosphorylation status.

We assayed the ubiquitin ligase activity of Ring1B/Mel-18 complex treated with AP. Whereas untreated Ring1B/Mel-18 or that treated with buffer alone ubiquitylated nucleosomes with similar high efficiency (Figure 6C, lanes 2 and 3), this was greatly diminished with the AP-treated complex (Figure 6C, lane 4). The E3 function of the MelPRC1 holocomplex purified from 293T cells showed a similar requirement for phosphorylation (Figure 6D). Importantly, the AP-treated Ring1B/Mel-18 complex retained the ability to ubiquitylate free histone proteins and also to carry out autoubiquitylation (Figure 6E, lanes 4–11 compared to lane 3), suggesting that, while E3 function is still intact, the complex was unable to recognize H2A lysine 119 in the context of the nucleosome substrate. Hence, the properties of the unphosphorylated Mel-18 directly mirror those of Mel-18^{C53G} mutant complex and suggest that, while phosphorylation does not enhance the intrinsic ubiquitin ligase function of the complex, it is required to promote recognition of the substrate.

DISCUSSION

In this study, we used affinity purification to identify human and mouse PRC1-like complexes containing MEL-18/Mel-18 (melPRC1). We show that, while melPRC1 shares common subunits with the previously described bmiPRC1, it is a functionally distinct complex. We demonstrate that melPRC1 represses *Hox* gene expression, and this correlates with its presence at the promoters of these genes. Ubiquitylation of H2A lysine 119 is associated with gene repression (Cao et al., 2005; de Napoles et al., 2004; Wang et al., 2004). In accordance, melPRC1 and a reconstituted subcomplex of melPRC1 comprising Mel-18 and Ring1B is an efficient E3 ligase in vitro and ubiquitylates H2A lysine 119 in chromatin. Mutation analysis reveals that while Ring1B plays a direct role in the ubiquitylation reaction, probably by mediating the interaction with the ubiquitin-conjugating enzyme, Mel-18 is critical for targeting the complex to lysine 119 of histone H2A in nucleosomes. Importantly, we find that, unlike bmiPRC1,